Received: 27 October 2023 | Revised: 29 January 2024 | Accepted: 5 March 2024

DOI: 10.1111/1541-4337.13329

Comprehensive REVIEWS in Food Science and Food Safety WILEY

COMPREHENSIVE REVIEW

Selenosugar, selenopolysaccharide, and putative selenoflavonoid in plants

Ziqi Qi[1] | **Alex Duan**[2] | **Ken Ng**[1]

[1]School of Agriculture, Food and Ecosystem Sciences, Faculty of Science, The University of Melbourne, Parkville, Victoria, Australia

[2]Melbourne TrACEES Platform, School of Chemistry, Faculty of Science, The University of Melbourne, Parkville, Victoria, Australia

Correspondence
Ken Ng, School of Agriculture, Food and Ecosystem Sciences, Faculty of Science, The University of Melbourne, Parkville, VIC 3010, Australia. Email: ngkf@unimelb.edu.au.

Abstract

Selenium (Se) is a naturally occurring essential micronutrient that is required for human health. Selenium supports cellular antioxidant defense and possesses bioeffects such as anti-inflammation, anti-cancer, anti-diabetic, and cardiovascular and liver protective effects arising from Se-enhanced cellular antioxidant activity. Past studies on Se have focused on elucidating Se speciation in foods, biofortification strategies to produce Se-enriched foods to address Se deficiency in the population, and the biochemical activities of Se in health. The bioavailability and toxicity of Se are closely correlated to its chemical forms and may exhibit varying effects on body physiology. Selenium exists in inorganic and organic forms, in which inorganic Se such as sodium selenite and sodium selenate is more widely available. However, it is a challenge for safe and effective supplementation considering inorganic Se low bioavailability and high cytotoxicity. Organic Se, by contrast, exhibits higher bioavailability and lower toxicity and has a more diverse composition and structure. Organic Se exists as selenoamino acids and selenoproteins, but recent research has provided evidence that it also exists as selenosugars, selenopolysaccharides, and possibly as selenoflavonoids. Different food categories contain various Se compounds, and their Se profiles vary significantly. Therefore, it is necessary to delineate Se speciation in foods to understand their impact on health. This comprehensive review documents our knowledge of the recent uncovering of the existence of selenosugars and selenopolysaccharides and the putative evidence for selenoflavonoids. The bioavailability and bioactivities of these food-derived organic Se compounds are highlighted, in addition to their composition, structural features, and structure–activity relationships.

KEYWORDS
organic selenium, selenium, selenoflavonoid, selenopolysaccharide, selenosugar

1 | INTRODUCTION

Selenium (Se) is a naturally occurring micronutrient that plays an important role in human health. Prior to 1950, it was widely believed that Se was toxic to humans and its research was limited by this perception. However, in the 1950s, Schwarz first discovered that Se has a protective effect on the liver when researching the causes of liver necrosis in rats maintained on highly purified casein diets. He found that the functional component was Se that had positive effects on the liver (Schwarz & Foltz, 1957). In the early 1970s, when Rotruck was studying the role of Se, he found that Se is a component of the antioxidant enzyme glutathione peroxidase, and in the case of Se deficiency, the activity of this enzyme cannot be fully expressed (Rotruck et al., 1973). This important study established Se as an essential element in maintaining a healthy body, by providing cellular antioxidant defense as glutathione peroxidase is a major antioxidant enzyme in all cells. In 1973, the World Health Organization (WHO) announced that Se is an essential trace element in the life activities of humans and animals. Since then, more in-depth research has been performed on Se to establish the relationship between Se-containing compounds and human health and the dietary requirement of Se and Se content from foods. The daily Se intake is variable according to the geographical source of the foods and the eating habits of the local populations. In Australia, dietary Se intake was reported to be 87 μg/day for men and 57 μg/day for women (Thomson, 2004); in the United States, it was reported to be 134 μg/day in men and 93 μg/day in women (Rayman, 2012), and in Europe, the dietary Se intake is located at a range of 40 to 60 μg/day in most regions (Ventura et al., 2017). The recommended dietary allowance for Se was eventually set at 55 μg/day for adult men and women over 19-year-old, and for women who are pregnant or lactating, it should be 60 and 70 μg/day by the WHO/FAO (Dong, Liu et al., 2021). The tolerable upper intake level (UL) for Se for all populations is 400 μg/day (Medicine, 2000). Selenium deficiency, which we now know, negatively impacts health, remains a worldwide challenge with approximately 0.5–1 billion people being affected by low Se intake and Se deficiency-related diseases including Keshan disease and Kashin–Beck disease. This is largely due to poor Se contents in many foods that are cultivated from Se-deficient soil (Pyrzynska & Sentkowska, 2021; Zhang et al., 2019). Additionally, the cooking process may have varying effects on the transformation and assimilation of selenium species present in food, such as the heating temperature can produce volatilization, degradation, and transformation of the species initially present in the raw food product (Alves et al., 2017; Dumont et al., 2006; Pedrero & Madrid, 2009; Pedrero et al., 2007; Pérez et al., 2018). Therefore, the Se intake level is not only dependent on the regional areas with different Se content in the soil but also on the cooking habits of the local people.

Selenium not only supports body antioxidant defense and immune response but also has a biological role in protecting thyroid function, anti-cancer, anti-diabetic, and cardiovascular protective effects arising from Se enhancing cellular antioxidant activity. However, an adequate dietary supplement of Se does not necessarily portend that the human body can absorb the total amount ingested (Dong, Liu et al., 2021; Khanam & Platel, 2016; Zagrodzki, 2022). The bioavailability of dietary Se ranges from 29% to 98% depending on the sources and Se forms (Arshad et al., 2021; Lei et al., 2022). Inorganic Se, such as sodium selenite (Na_2SeO_3) and sodium selenate (Na_2SeO_4), is much more readily available in foods and at higher levels due to their cost-effectiveness, for example, added to animal feed (Liao et al., 2011). There is the application of selenium nanoparticle (SeNP) as a nutritional supplement, which can be synthesized through chemical, biological, and physical methods by combining inorganic Se species with other biological compounds (Nayak et al., 2021). Given that the reported toxicity of elemental Se (Se^0) in nano size is comparatively lower than that of selenate (Se^{II}), selenite (Se^{IV}), or selenate (Se^{VI}) ions, SeNPs emerge as a viable option for substituting other Se forms in clinical settings (Ferro et al., 2021; Skalickova et al., 2017; Wadhwani et al., 2016). However, it is still a challenge for safe and effectual supplementation considering inorganic Se low bioavailability, high cytotoxicity, and short retention time in the gastrointestinal tract. Numerous evidence indicated that organic Se from foods is more effective than inorganic Se in providing antioxidant protection to cells and tissues and that organic Se exhibited higher bioavailability and much lower toxicity, and different organic Se forms may possess different bioactivity and bioavailability that may have varying effects on the body physiology (Feng et al., 2021; Gandin et al., 2018; Jiang et al., 2022, 2021; Rua et al., 2023). The assimilation of inorganic Se present in the soil may occur within plants through its substitution for the sulfur atom in amino acids, thereby giving rise to selenoamino acids like selenomethionine, selenocysteine, methylselenocysteine, and selenoneine. Subsequent transformations of these selenoamino acids lead to the formation of selenoproteins. It is noteworthy that the health protective effects attributed to Se are contingent not only upon its concentration acquired through dietary sources but also on specific chemical forms. There is a need to enlarge the organic Se pool available to the human diet in addition to the well-known selenoamino acids and selenoproteins, to discover and explore more organic Se species with different biological properties with health properties.

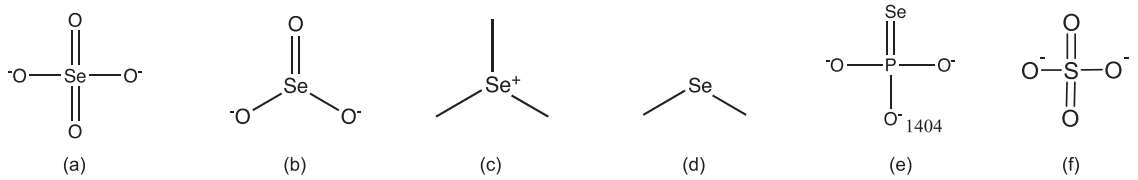

FIGURE 1 Structure of some organic and inorganic Se and S chemical forms. (A) Selenate (SeO_4^{2-}), (B) selenite (SeO_3^{2-}), (C) trimethylselenonium ($(CH_3)_3Se^+$), (D) dimethyl selenide ($(CH_3)_2Se$), (E) selenophosphate (PO_3Se^{3-}), and (F) sulfate (SO_4^{2-}).

Overall, a comprehensive knowledge of the Se content is still lacking, Se distribution, bioconversion, and speciation in many agricultural and food products are not well studied, and even less about the health benefits and toxicities of organic Se compounds in many naturally occurring Se-containing products. It is insufficient to recommend a healthy diet solely based on the total Se content of food as Se species exhibit different physicochemical characteristics and biological effects. Thus, increasing attention has been paid to the cultivation and preparation methods of Se-biofortified foods, the organic Se species found in foods, as well as their associated health benefits. Recently, the discovery of new organic-Se species made these tasks even more imperative. This review highlights these new findings by covering the current research on the discovery, composition, and structural features of selenosugars, selenopolysaccharides (SePSs), and putative selenoflavonoids (SeFs) from foods, and summarizes their bioavailability, biological activities, and structure–activity relationships.

2 | SELENOSUGAR AND SELENOPOLYSACCHARIDE

Since selenosugars are metabolic products of Se in mammalian cells, it points to the possibility of the existence of similar compounds in plants (Hildebrand et al., 2020; Kobayashi et al., 2002; Lajin et al., 2016). Indeed, the existence of Se-containing monosaccharides and disaccharides in edible plants was only documented recently. In addition, the fact that sulfated polysaccharides are found in plants might also indicate the possibility of SePS existence since both sulfate and H_2SeO_4 are oxyanions chalcogens and share many chemical properties on account of their similar outer electronic configurations (Figure 1). Indeed, recent research was successful in identifying SePS in some plants and fungi, and such compounds have improved bioactivity compared to Se-free polysaccharides from the same sources. This finding enlarged the organic Se pool available to the human diet in addition to the well-known selenoamino acids and selenoproteins. Selenopolysaccharides are more complex molecules compared to selenosugars. They are long-chain polymers made up of sugar units with Se atoms incorporated into their structure. Once the structure and bioeffects of SePSs have been elucidated, it may be possible to apply them in the development of nutraceutical products beneficial to human health.

2.1 | Identification of selenosugar

Table 1 presents a summary of various selenomonosaccharides (SeMSs) and selenodisaccharides (SeDSs) identified to date, in terms of their sources, proposed structure and molecular formula, and the corresponding detection methods in elucidating their structures.

Aureli et al. (2012) first identified some selenosugars by high-performance liquid chromatography–electrospray ionization orbitrap tandem mass spectrometry (HPLC-ESI-Orbitrap-MS), in which structures included diamino selenocysteine-Se-hexose, cyclic selenomethionine-Se-hexose, methylseleno-Se-pentose-hexose, and methylseleno-Se-deoxypentose-hexose in wheat (*Triticum aestivum*), rice (*Oryza sativa*), and maize (*Zea mays*). This was followed by Ouerdane et al. (2013) in confirming the existence of the same selenosugars, also by HPLC-ESI-Orbitrap-MS, in black mustard seeds (*Brassica nigra*) and the discovery of three new monosaccharides that are covalently bound to another compound. These selenosugar structures indicate that the incorporation pattern of Se can occur: (a) by acylation of the glucose hydroxyl group, such as by acylation of Se-sinapinic acid metabolite of sinapine to form methyl selenosinapoylsinigrin or (b) by substitution of the S atom with Se as in Se-glucosyl-Se-allyl-*N*-hydroxy-selenourea.

Selenium-containing disaccharide was also recently reported in kale sprouts by Zagrodzki (2022) by zwitterionic-type hydrophilic interaction liquid chromatography–electrospray ionization mass spectrometry (ZIC-HILIC-ESI-MS). In addition to the natural selenosugar, Se-containing sucrose (sucrose selenious ester) has been synthesized by Guo et al. (2013), and its molecular structure was characterized by carbon-13 nuclear magnetic resonance (^{13}C-NMR) and Fourier transform infrared spectroscopy (FT-IR. The FT-IR showed that

TABLE 1 Selenosugar, corresponding masses, empiric formulas, and proposed structures.

Detected molecules	Present in	Identification method	Theoretical mass (*m/z*)	Experimental mass (*m/z*)	Error (ppm)	Proposed molecular formula	Proposed structure	Reference
$[M + NH_4^+]$ ion, Selenosugar	Rice, maize, and wheat	HPLC-ICP-MS, HPLC-ESI-Orbitrap MS(/MS)	407.04546	407.04500	1.13	$C_{12}H_{23}O_{10}Se^+$ Methylseleno-Se-pentose-hexose	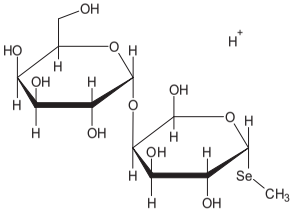	Aureli et al. (2012)
Selenosugar	Rice, maize and wheat		408.07674	408.07725	−1.25	$C_{12}H_{26}NO_9Se^+$ Methylseleno-Se-deoxypentose-hexose	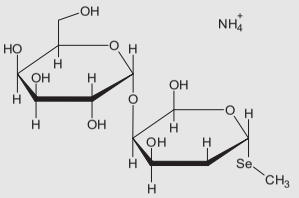	
Selenosugar	Rice, maize		317.01341	317.01346	−0.16	$C_9H_{17}O_7Se^+$ Deamino selenocysteine-Se-hexose	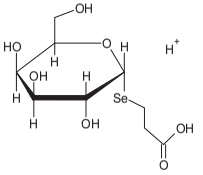	
Selenosugar	Maize		358.04001	358.03998	0.08	$C_{11}H_{20}NO_7Se^+$ Cyclic selenomethionine-Se-hexose	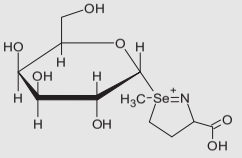	
$[M + NH_4^+]$ ion, Selenosugar	Seeds of *Brassica nigra*	HILIC-ICP-MS, HPLC-ICP-MS, HPLC-ESI-Orbitrap MS(/MS)	408.07674	408.07698	0.6	$C_{12}H_{26}NO_9Se^+$ Methylseleno-Se-deoxypentose-hexose	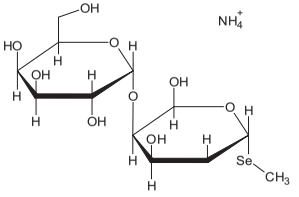	Ouerdane et al. (2013)

(Continues)

TABLE 1 (Continued)

Detected molecules	Present in	Identification method	Theoretical mass (*m/z*)	Experimental mass (*m/z*)	Error (ppm)	Proposed molecular formula	Proposed structure	Reference
Selenosugar	Seeds of *Brassica nigra*		407.04546	407.04474	−1.8	$C_{12}H_{23}O_{10}Se^{+}$ Methylseleno-Se-pentose-hexose	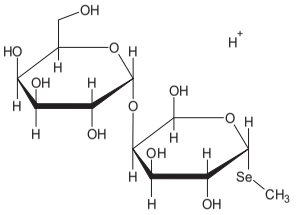	
Selenosugar	Seeds of *Brassica nigra*		343.04029	343.04023	−0.2	$C_{10}H_{19}N_2O_6Se$ Se-glucosyl-Se-allyl-*N*-hydroxy-selenourea	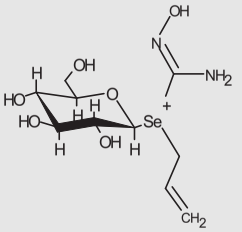	
Selenosugar	Seeds of *Brassica nigra*		304.02939	304.02917	−0.7	$C_8H_{18}NO_6Se$ 5'-3-Selenylpropanoic acid-ribofuranose	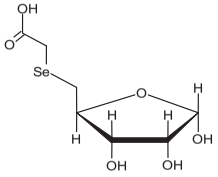	
Selenosugar	Seeds of *Brassica nigra*		660.03303	660.03298	0.1	$C_{22}H_{30}NO_{13}S_2Se$ Methylselenosinapoylsinigrin	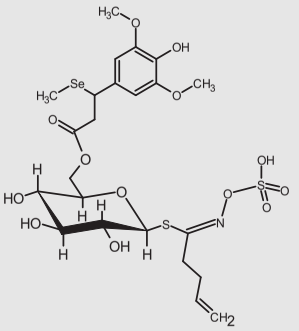	
Selenosugar	Kale sprouts	HPLC-ICP-MS, ZIC-HILIC-ESI-MS	389.0356	389.0359	0.701	$C_{12}H_{21}O_9Se^{-}$ Methylseleno-Se-deoxypentose-hexose	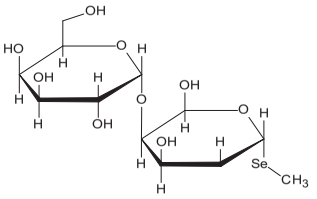	Zagrodzki et al. (2022)

(Continues)

TABLE 1 (Continued)

Detected molecules	Present in	Identification method	Theoretical mass (*m/z*)	Experimental mass (*m/z*)	Error (ppm)	Proposed molecular formula	Proposed structure	Reference
			Se bond and wavelength					
Selenosugar	Selenized sucrose	^{13}C-NMR, FT-IR	Se=O (925 cm^{-1}), Se-OH (681 cm^{-1})			$C_{12}H_{22}O_{12}Se$ Sucrose selenious ester		Guo et al. (2013)

Abbreviations: HPLC, high-performance liquid chromatography; HILIC, hydrophilic interaction liquid chromatography; ICP, inductively coupled plasma; MS, mass spectrometry; ESI, electrospray ionization; ZIC-HILIC-ESI-MS, zwitterionic-type hydrophilic interaction liquid chromatography electrospray ionization mass spectrometry; HPLC-ESI-Orbitrap MS(/MS), HPLC-electrospray ionization orbitrap tandem mass spectrometry; FT-IR, Fourier transform infrared spectrum; NMR, nuclear magnetic resonance.

there were two new absorption peaks at 681 and 925 cm^{-1}, which were related to the bonds of Se-OH and Se = O, respectively, and in the MTT (3-(4,5-dimethylthiazol-2-yl)−2,5-diphenyl-2H-tetrazolium bromide) assay, Se-containing sucrose demonstrated dose-dependent cytostatic effects on human hepatocellular carcinoma cells (SMMC-7221). Notably, it did not exert adverse effects on the proliferation of human normal hepatic cells (HL-7702) within the concentration range of 0.15 to 1.2 ppm Se. This highlights its capacity to selectively hinder the growth of cancerous cells while sparing healthy ones. The use of morphological observations, agarose gel electrophoresis, and caspase-3 assays revealed that Se-containing sucrose prompted mitochondrial apoptosis in SMMC-7221 cells. This was corroborated by the observation of a decline in mitochondrial membrane potential and the inhibition of caspase-3 activity. These findings underscore the potential of Se-containing sucrose in inducing apoptosis in cancer cells, rendering selenosugars as promising candidates for the development of anticancer drugs.

However, it should be noted that the exact structures of many putatively identified selenosugars in plant materials using less vigorous analytical methods remain speculative. The challenge in structural identification arises from the presence of numerous naturally occurring polysaccharides within the plant matrix, all of which could potentially incorporate Se and result in a wide range of possible structures. Thus, more studies are needed to detect these selenosugars and to determine their structures with more certainty, as this knowledge is essential in understanding SePS synthesis and in advancing the application of these compounds in human health.

2.2 | Possible mechanisms for the biosynthesis of selenosugar

There are two possible mechanisms for the synthesis of selenosugar in plants, namely, by enzymatic or chemical means. Glycosylation of plant secondary metabolites catalyzed by glycosyltransferases (GTs) is a common enzyme modification reaction that can affect the bioactivity, stability, solubility, and transport of these compounds (Berthiller et al., 2006; Cooper et al., 2001). For example, GTs could facilitate the glycosylation of thiol species, such as in the production of glucosinolates in plants (Blazevic et al., 2020; Petersen et al., 2019), indicating the possibility of similar glycosylation pathways for selenol groups considering the similar chemical properties of sulfur and Se. Chemically driven oxidative reactions of Se-containing compounds with sugars can also lead to the production of selenosugars where the Se can be incorporated into the anomeric carbon of the sugar ring. Such a reaction would involve the

incorporation of Se from selenoamino acids or methylselenol, and the formed selenosugars could then be fed into polysaccharide synthesis (Ouerdane et al., 2013). For example, xyloglucan is a polysaccharide synthesized in the Golgi apparatus in plant cells. The backbone of xyloglucan is composed of β-(1,4)-linked glucose residues, most of which are substituted with a xylose residue as the sidechain in an α-(1,6)-linkage. The branched entity (xylose) can be further decorated with various glycosyl groups, for instance, β-(1,2)-linked galactose followed by α-(1,2)-linked fucose, or can be further capped with β-(1,2)-linked glucuronic acid followed by β-(1,4)-linked galactose (Mikkelsen et al., 2021). Indeed, Aureli et al. (2012), Ouerdane et al. (2013), and Zagrodzki (2022) identified Se-containing disaccharide compounds in rice, maize, wheat, black mustard seeds, and kale sprouts exhibiting this pentose–hexose structure with methylselenol linked to C1 of the reducing pentose pyranose ring of the disaccharide (Table 1). This disaccharide could be generated from xyloglucan, in which the glucose with an attached xylose side chain is also in a hexose–pentose pyranose form. On the contrary, enzymatical glycosylation incorporating the selenol group would result in the addition of the Se on the hexose moiety (glucose) of this disaccharide (Aureli et al., 2012; Mizutani et al., 2002). Selenosugar with different structures can be explained by these two possible biosynthesis mechanisms; however, further research is needed to figure out and provide strong scientific evidence of the mechanisms of selenosugar biosynthesis.

2.3 | Se forms on selenopolysaccharide

Although Se and sulfur share similar outer electron shell configurations, this does not mean that their present forms on polysaccharides are similar, which is reflected in their valence states and binding sites on the sugar structure. Sulfated polysaccharides are present in mammals, algae (Chen et al.,2023; Yang et al., 2011), fungi (Chang et al., 2013), and some plants such as pine pollen (Geng et al., 2016), ginseng (Ragab et al., 2018), and tea (Wang, Shi et al., 2013). All these sulfate polysaccharides have S in a sulfate group (R-O-S[O_2]-OH) attached to the sugar entity linked by an oxygen atom in an ether linkage; the S is in the +6-oxidation state and thus non-reducing. It is tempting to speculate that Se might also exist as the selenate group (R-O-Se[O_2]-OH) on sugar in a similar oxygen linkage, the Se similarly in +6-oxidation state and thus also non-reducing (Figure 1). However, based on the results of the current exploration of SePS, Se mainly exists as selenite on polysaccharides in the Se^{4+}, as selenoglycosides in the Se^{2+} form (Raics et al., 2022), or with Se replacing oxygen in the sugar ring (Górska et al., 2021) (Figure 2).

The reactivity of hexose's hydroxy group is known and is in the order of C-6 > C-2 > C-4 (Yang et al., 2005). This is shown in the sulfated polysaccharides isolated from *Gynostemma pentaphyllum* where analysis by FT-IR and ^{13}C-NMR shows that the sulfated groups were mainly linked to the C-6 position with some to the C-2 position of the sugars (Chen et al., 2011). Structural investigations by FT-IR and Raman spectroscopy and ^{1}D/^{2}D-NMR of chemically synthesized SePS using green tea PS and sodium selenite (Na_2SeO_3) showed that the Se is chemically incorporated in the form of the selenyl ether (R-O-Se[O]-OH) at the C-6 position of the sugars (Figure 2A) (Zhu, Yu et al., 2020). However, in SePS isolated from tea, Se replaced some of the sugar hydroxyl groups at the C-1 and C-6 positions on the polysaccharide branched sugars and contained the -SeH chemical form (Figure 2B) (Zhu, Yu et al., 2020). This chemical form is similar to the -SH thiol group and is reducing. Thus, the Se form obtained by the biosynthetic route is different from the selenyl ether obtained by the chemical route. It may be that selenylation as in sulfation does not occur naturally. Therefore, although sulfated polysaccharides point to the possibility of the presence of SePS, the Se forms in SePS cannot be inferred from information about sulfated polysaccharides alone. Unlike the non-reducing H_2SeO_4 group, the Se in the H_2SeO_3 group is in the Se^{4+} oxidation state and thus is a reducing group. Structural analyses are required to confirm the Se forms on polysaccharides, and further studies are needed to explore the ways Se binds to sugar molecules.

2.4 | Source and isolation or synthesis of selenopolysaccharide

At present, SePS can be obtained naturally from agriculture plants grown in Se-rich soil, henceforth referred to as natural SePS, but the SePS content from such sources is relatively low, which limits research and development. Therefore, "enrichment" means has been employed in obtaining higher levels of SePS in tea, bacteria, fungi, or algae through inorganic Se fortification of the growth medium; henceforth, we refer to these as enriched SePS (Dong, Xiao et al., 2021; Kaleta et al., 2019; Zhang et al., 2020, 2022; Zhou et al., 2020). These two Se sources need to be distinguished because there are differences between natural and enriched SePS in terms of their structural characteristics, biological activities, as well as the Se forms in the polysaccharides. In addition, chemical selenylation of polysaccharides with Na_2SeO_3 has also been employed to obtain SePS with an added selenite group for investigation, and these are referred to as synthetic SePS (Chen & Huang, 2018).

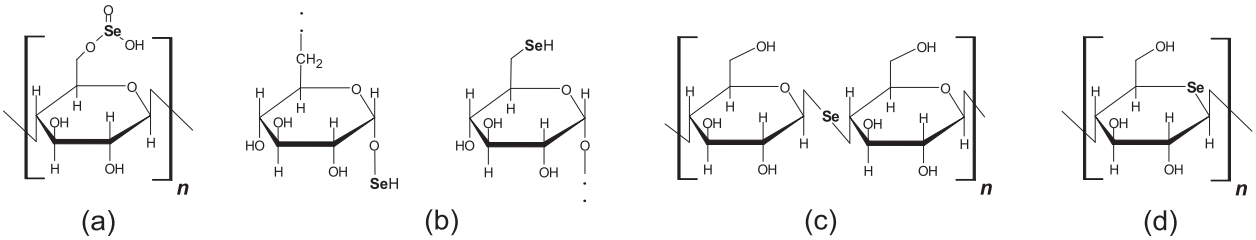

FIGURE 2 Possible Se forms on sugars in Se-containing polysaccharides. (A) -$HSeO_3$ at C-6 position; (B) -SeH at C-1 or C-6 position; (C) C-Se-C in glycosidic linkage; (D) Se replaces O in sugar pyranose ring.

2.4.1 | Natural and enriched selenopolysaccharide

Plants are one of the main sources of natural SePS (Table 2). Plant SePSs have been isolated from *Rosa laevigata* Michx fruits from Bozhou (Anhui, China) (Liu et al., 2022), pennycress (*Thlaspi arvense* L.) (Xiang et al., 2022), and tea leaves grown in some Se-rich regions, including tea leaves from Enshi (Hubei, China) (Cheng et al., 2018; Zhu et al., 2019), Yichang (Hubei, China) (Zhu, Yu et al., 2020), and Pingli and Ziyang (Shaanxi, China) (Gu et al., 2020; He et al., 2013; Zhao et al., 2022) regions.

The biosynthesis of SePS in plants can be affected by the Se forms and concentrations in soil, as well as the Se absorption pathways and anabolism in plants. Typically, Se at a concentration from 1 to 10 mg/kg dry weight can stimulate the growth and increase stress resistance of plants, and a toxic level is reached when the Se concentration in plant tissue is over 100 mg/kg dry weight (Pilon-Smits, 2019), but Se accumulation and tolerance capacities vary greatly between different plant species, and for some Se hyperaccumulators, the tolerance limit can reach 1000−15,000 mg/kg dry weight (Pilon-Smits, 2019).

Although the specific transport systems for the biosynthesis of SePS in plants have not yet been fully unraveled, it was found that the transport and accumulation of Se are linked to the overexpression of the sulfate transporters SULTR1 and SULTR2 (El Mehdawi et al., 2018), as well as to the overexpression of phosphorus transporter OsPT2 (Zhang et al., 2014). The absorption into plants and transport rate within the plants can be influenced by the Se form. The Se forms present in soil included: (i) soluble Se salts such as sodium selenate (Na_2SeO_4) and selenite (Na_2SeO_3), (ii) exchangeable and carbonate-bound Se, (iii) Fe/Mn oxide-bound Se, (iv) organic matter-bound Se or organic Se, and (v) residual Se fraction that is strongly retained by soil particles (Wang, Liang et al., 2012). The soluble and exchangeable Se, which accounts for less than 1% of total Se in the upland soil and around 16.1% in the paddy soil (Wang, Liang et al., 2012), is considered the most bioavailable to plants (Hu et al., 2014). Fe/Mn oxide-bound Se is more commonly found in upland soil, whereas organic matter-bound Se is the predominant Se fraction in paddy soil. Soluble Se oxidation state species in upland soil included Se^{2-}, Se^{4+}, and Se^{6+}. It was found that Se^{6+} had a significant direct effect on the accumulation of Se in corn (*Z. mays* L.), but the organic matter-bound Se could significantly affect the Se accumulation indirectly, which is believed as an important fraction and source of plant Se in soil (Wang, Shi et al., 2013; Wang, Liang et al., 2012).

The Se content in SePS varies with different agricultural regions, where they have different available Se content in soil, and differs in plant species. Tea presents an easily available source of SePS. Natural SePS isolated from green tea grown in Ziyang region (Shaanxi province, China) was found to have a Se content of 2.14 μg/g SePS (Y. Wang et al., 2013). Tea grown in other regions in China has differing Se content in the isolated polysaccharides, reflecting the Se content of the cultivation soils. Tea grown in the Pingli region (a county close to Ziyang in Ankang City, China) has Se content in the range of 5.59–23.50 μg/g SePS (Gu et al., 2020; Zhao et al., 2022), those from Enshi (Hubei province, China) ranges from 0.34 to 2.76 μg/g (Cheng et al., 2018; Wang et al., 2015; Zhu et al., 2019), and those from Yichang (a city close to Enshi) about 1.64 μg/g (J. Zhu et al., 2020). Besides tea, natural SePSs have also been isolated from pennycress (*T. arvense* L.) with a Se content of 13.56–15.36 μg/g (Xiang et al., 2022), and from Michx fruits (*R. laevigata*), a much higher Se content ranging from 16.49 to 21.61 μg/g was found (Liu et al., 2022).

Se fortification of growth medium and soil has been employed to obtain a higher yield of biosynthesized SePS from various sources. These enriched SePS can differ from natural SePS in terms of their molecular weight (MW) and the Se content of the SePS. Enriched SePSs have been obtained from fungi and algae that included *Cordyceps militaris* (Ren et al., 2020), *Catathelasma ventricosum* (Liu et al., 2013), *Grifola frondosa* (Huang et al., 2020; Q. Li et al., 2017), *Pleurotus ostreatus* (Zhang et al., 2020, 2022, 2021), *Pleurotus geesteranus* (Sun et al., 2017), *Phellinus igniarius* (*Luo* et al., *2021*), *Lentinula edodes* (Kaleta et al., 2019; Malinowska et al., 2018), *Fomes fomentarius* (Keshavarz-Rezaei et al., 2022), *Spirulina platensis* (Zhou et al., 2020), *Flammulina velutipes* (Dong, Xiao et al., 2021), *Oudemansiella*

TABLE 2 Structural characterization of selenopolysaccharides.

SePS	Study objects	Se source	Se content in SePS (μg/g)	Mw (Da)	Monosaccharide composition and molecular ratio	Se bond and wavelength (cm^{-1})	Glycosidic linkage or conformation	Analysis method	Reference
SeTP	Tea	Natural	7.93 ± 0.14 (SeTPS-1); 5.59 ± 2.28 (SeTPS-2); 6.00 ± 2.93 (SeTPS-3)	4.70×10^4 (SeTPS-1); 4.36×10^4 (SeTPS-2); 3.49×10^4 (SeTPS-3);	SeTPS-1: Man, Glc, Gal, Xyl, and Ara (1.01:3.59:0.21:1.14:0.19); SeTPS-2: Man, GlcA, Glc, Gal, Xyl, and Ara (2.85:0.68:9.70:0.93:2.00:0.87); SeTPS-3: Man, GlcA, Glc, Gal, and Xyl (1.38:0.34:15.30:0.18:1.28)	Se-O-C (676 cm^{-1}) O-Se-O (1050 cm^{-1}) Se = O (799 cm^{-1})	*β*-glycosidic linkage	Purification: DEAE-cellulose 52 column and Sephadex G-100 column Se detection: AFS Structure characterization: GPC; UV; HPLC; FT-IR; SEM	Zhao et al. (2022)
SeZYTP	Tea	Natural	2.14	/	Man, Rha, and fuc (2.4:1.5:1.2:0.2:0.1:0.3:0.3)	/	/	Purification: DEAE-Sepharose Fast Flow column and Sephacryl S-400/HR column Se detection: AFS Structure characterization: GC; HPSEC	Y. Wang et al. (2013)
SeTPSs	Tea	Natural	0.97 (SeTPS1); 0.44 (SeTPS); 0.34 (SeTPS3)	1.1×10^5 (SeTPS1); 2.4×10^5 (SeTPS2); 9.2×10^5 and 2.5×10^5 (SeTPS3);	SeTPS1: Fuc, Rha, Ara, Gla, Glc, GlcA (0.07:0.21:0.58:1.00:0.47:0.17:1.75); SeTPS2: Fuc, Rha, Ara, Gla, Glc, GlcA (0.07:0.28:0.59:1.00:0.10:0.49:1.24); SeTPS3: Fuc, Rha, Ara, Gla, Glc, GlcA (0.07:0.38:0.72:1.00:0.300.19:0.88)	/	/	Purification: DEAE-Sepharose Fast Flow column Se detection: AFS Structure characterization: HPGPC; IC; FT-IR; SEM; AFM	Wang et al. (2015)
SeTPS	Tea	Natural	2.76 ± 0.10	/	/	/	/	Se detection: AFS	Cheng et al. (2018)
SeTPSs	Tea	Natural	23.50 (SeTPS-1); 13.47 (SeTPS-2)	1.70×10^4 (SeTPS-1); 1.30×10^4 (SeTPS-2)	SeTPS-1: Glc, Gal (80.1:2.3); SeTPS-2: Ara, Glc, Gal, GalA (2.04:48.83:3.21:1.30)	O-Se-O (1025 cm^{-1}) Se = O (763 cm^{-1})	*α*-glycosidic bond-linked Glc*p*; random coil conformation	Purification: DEAE-cellulose 52 column and Sephadex G-100 column Se detection: AFS Structure characterization: HPGPC; GC; SEM; AFM; FT-IR; NMR; Congo red test	Gu et al. (2020)

(Continues)

TABLE 2 (Continued)

SePS	Study objects	Se source	Se content in SePS (μg/g)	Mw (Da)	Monosaccharide composition and molecular ratio	Se bond and wavelength (cm^{-1})	Glycosidic linkage or conformation	Analysis method	Reference
ASe-TPS1 CSe-TPS1	Se-enriched; artificial Se-enriched tea	Na_2SeO_3-fortified cultivation (ASe-TPS1); NA-SS (CSe-TPS1)	1.64 ± 0.48 (ASe-TPS1); 2.12 ± 0.24 (CSe-TPS1)	/	ASe-TPS1: Rha, Ara, Gal, Glc, Xyl, Man, Frc, and GalA (0.16:0.25: 0.76:1.00:0.05: 0.10:0.12:0.31); CSe-TPS1: Rha, Ara, GlcNAc, Gal, Glc, Xyl, Man, Frc, and GalA (0.15:0.90:0.12:1.54:1.00:0.21:0.67:0.20:0.01)	FT-IR: Se-O-C (611 cm^{-1}) O-Se-O (1080 cm^{-1}) Se-H (669 cm^{-1}) Raman spectra: Se-O-C (791, 632 cm^{-1}) Se-OH (664 cm^{-1}) Se = O (742 cm^{-1}) Selenylation occur at C-1 and C-6 position, and may occur at C-3	α-$_L$-glycosidic linkage and β-$_D$-glycosidic linkage	Purification: DEAE-Sepharose Fast Flow column Se detection: AFS Structure characterization: IC; FT-IR; Raman spectroscopy; Congo red test; NMR; SEM; I_2-KI test; x-ray diffraction; DSC	J. Zhu et al. (2020)
ASe-TPS2 NSe-TPS2	Se-enriched tea; artificial Se-enriched tea	Na_2SeO_3 fortified cultivation (ASe-TPS2); Natural (NSe-TPS2)	0.75 ± 0.10 (ASe-TPS2); 0.44 ± 0.10 (NSe-TPS2)	6.73×10^3 (ASe-TPS2); 2.44×10^5 (NSe-TPS2)	ASe-TPS2: Rha, Ara, Glc, Xyl, and Gal (1.93:7.05:1.00:1.05:26.12); NSe-TPS2: Fuc, Rha, Ara, Gal, Glc, GlcA, and GalA (0.07:0.28:0.59:1.00:0.10:0.49:1.24)	/	Nse-TPS2: 1,4-β-D-Glc*p*, 1,4-α-D-Gal*p*A; branch: 1,2-β-L-Ara*f*, 1,3-α-D-Gal*p*, and 1,2-β-L-Rha*p*; non-reducing ends: Glc*p* and Cal*p* residues. ASe-TPS2: 1,3-β-D-Glc*p*, 1,4-α-D-Gal*p*A,1,4-Glc*p*, 1,2-α-L-Rha*p*; non-reducing ends: Ara*f* and Xyl*p*	Purification: DEAE-Sepharose Fast Flow column Se detection: AFS Structure characterization: HPGPC; IC; FT-IR; NMR; SEM; Methylation analysis (GC-MS)	Zhu et al. (2019)
Se-RLFPs	Michx fruits (*Rosa laevigata*)	Natural	16.49 ± 0.12 (Se-RLFP-I); 21.61±0.47 (Se-RLFP-II)	2.40×10^4 (Se-RLFP-I); 1.60×10^4 (Se-RLFP-II)	Se-RLFP-I: Rha, Xyl, and Glc (0.12:0.51:0.39); Se-RLFP-II: Rha, Xyl, and Glc (0.39:0.44:0.17)	Se-O-C (620.98, 617.12 cm^{-1}) Se = O (761.76, 760.89 cm^{-1})	1, 3 glycosidic linkages	Purification: DEAE-cellulose 52-column and Sephadex G-200 column Se detection: AFS Structure characterization: HPGPC; HPLC; FT-IR; NMR; SEM; TGA	Liu et al. (2022)
Se-PPSs	Pennycress (*Thlaspi arvense* L.)	Natural	13.56 ± 1.87 (Se-PPS1); 15.36 ± 2.30 (Se-PPS3)	4.20×10^4 (Se-PPS1); 4.50×10^4 (Se-PPS3)	Se-PPS1: Glc, Gal, and Ara (0.95:0.03:0.02); Se-PPS3: GluA, Rha, GalA, Glu, Gal, Xyl, and Ara (0.17:0.03:0.08:0.31:0.22:0.06:0.13)	O-Se-O (762, 777 cm^{-1}) Se = O (1028, 1045 cm^{-1})	1,6-ß-$_D$-Gal*p* and T-α-$_D$-Glc*p* configurations	Purification: DEAE-cellulose 52 column and Sephadex G-100 column Se detection: AFS Structure characterization: GPC; HPLC; UV; FR-IR; GC-MS; NMR; Methylation analysis (GC-MS)	Xiang et al. (2022)

(Continues)

TABLE 2 (Continued)

SePS	Study objects	Se source	Se content in SePS (μg/g)	Mw (Da)	Monosaccharide composition and molecular ratio	Se bond and wavelength (cm^{-1})	Glycosidic linkage or conformation	Analysis method	Reference
Se-L	*Lentinula edodes*	Na_2SeO_3 fortified cultivation	190	2.61×10^5	Man and Glc (1:6)	Se (II) is probably glycosidically bound in β-1,3- or α-1,4-glycosidic bonds, or substituted for oxygen in the carbohydrate acetal ring	1, 6-β-$_D$-glucan with some branching points at O-3	RP HPLC; FT-IR; HPGPC; NMR; XAS; EXAFS	Kaleta et al. (2019) and Malinowska et al. (2018)
Se-F	*Flammulina velutipes*	Na_2SeO_3 fortified cultivation	108	/	/	/	/	Se detection: AFS Structure characterization: ICP-MS; HPLC-ICP-MS	Dong, Xiao, et al. (2021)
Se-SPP	*Spirulina platensis*	Na_2SeO_3-fortified cultivation	14.12 ± 1.41	4.52×10^4	Man, Rha, and Glc (0.21:1.02:98.77)	/	/	Se detection: ICP-MS Structure characterization: GPC; HPLC; FT-IR; SEM	Zhou et al. (2020)
Se-POP-3	*Pleurotus ostreatus*	Na_2SeO_3 fortified cultivation	25.9	1.6106×10^4	Man, Glc, and Gal (1.7:49.6:2.4)	C-O-Se (660 cm^{-1}) Se = O (758 cm^{-1})	Both α-glycosidic linkage and β-glycosidic linkage	Purification: DEAE-cellulose 52 Se detection: ICP-AES Structure characterization: HPGPC; Congo red test; HPLC; FT-IR; NMR; DLS; AFM; TEM	Zhang et al. (2020) and Y. Zhang et al. (2022)
Se-POP-1	*Pleurotus ostreatus*	Na_2SeO_3-fortified cultivation	3.69	1.62×10^4	Glc, Man, and Gal (5.30:1.55:2.14)	C-O-Se (941 cm^{-1}) Se = O (1048 cm^{-1})	/	Purification: DEAE-cellulose 52 column and Sephadex G-100 column Se detection: AAS Structure characterization: HPGPC; FT-IR; GC; SEM	Ma et al. (2022)
Se-POP-21	*Pleurotus ostreatus*	Na_2SeO_3-fortified cultivation	5.31	1.5888×10^4	Man, Glc, Gal, and Ara (18.01:2.40:26.15:7.34)	Se-O-C (654 cm^{-1}) Se = O (756 cm^{-1})	Both α-glycosidic linkage and β-glycosidic linkage	Purification: DEAE-cellulose 52 column and Sephadex G-100 column Se detection: AFS Structure characterization: HPGPC; Congo red test; HPLC; FT-IR; NMR; DLS; AFM; TEM	Zhang et al. (2021)
SPMP-2a	*Pleurotus geesteranus*	Na_2SeO_3-fortified cultivation	/	3.32×10^4	/	/	α-$_D$-glucopyranoside linkage	Purification: DEAE Sepharose Fast Flow column and Superdex-200 column Structure characterization: FT-IR	Sun et al. (2017)

(Continues)

TABLE 2 (Continued)

SePS	Study objects	Se source	Se content in SePS (μg/g)	Mw (Da)	Monosaccharide composition and molecular ratio	Se bond and wavelength (cm^{-1})	Glycosidic linkage or conformation	Analysis method	Reference
PSeP	*Phellinus igniarius*	Na_2SeO_3-fortified cultivation	120.00	3.212×10^6	Man, Rib, GlcA, Glu, Gal, and Ara (1:0.15:0.45:1.87:2.11:0.05)	O-Se-O (919.87 cm^{-1}) Se = O (460 cm^{-1}) Se-H (670 cm^{-1})	α-anomeric configuration and β-anomeric configuration (α-$_D$-Man*p*, α-$_D$-Glc*p*, and β-$_D$-Gal*p*)	Purification: DEAE-cellulose 52 column Se detection: AFS Structure characterization: GC; HPGPC; FT-IR; NMR	Luo et al. (2021)
Se-CMP	*Cordyceps militaris*	Na_2SeO_3-fortified cultivation	/	2.021×10^6	/	O-Se-O (977.25 cm^{-1}) Se = O (891.43 cm^{-1})	/	Purification: Sephadex G-100 column Structure characterization: FT-IR; SEM; HPGPC	Ren et al. (2020)
Se-GFP-22	*Grifola frondosa*	Na_2SeO_3-fortified cultivation	8.37	4.13×10^6	Man, Glc, and Gal (3.3:23.3:1)	Se-O-C (667.9 cm^{-1}) O-Se-O (1024.5 cm^{-1}) Se = O (759.9 cm^{-1})	Main chain: 1,4-α-$_D$-Glc*p* units with a branch at C-6 of both 1,3,6-β-$_D$-Man*p* and 1,4,6-α-$_D$-Gal*p* units. Side chains: 1,4-α-$_D$-Glc*p* oligosaccharides and terminated by α-$_D$-Glc*p* units.	Purification: DEAE-cellulose 52 column and Sephacryl S-400 Superfine column Se detection: AFS Structure characterization: FT-IR; GC; GC-MS; NMR; HPSEC-MALI-RI; Congo red test; AFM, SEM	Q. Li et al. (2017)
SPS	*Oudemansiella radicata*	Na_2SeO_3-fortified cultivation	127.1	3.12×10^4	Rib, Man, Gal, and Glc (2.5:3.0:25.2:25.3)		α-glycosidic linkage	Se detection: AAS Structure characterization: GC; UV; HPGPC; FT-IR; NMR	Gao et al. (2018)
SPC-2	*Catathelasma ventricosum*	Na_2SeO_3-fortified cultivation	41.77	1.6×10^5	Glucose (87.4%)		β-glucan structure	Purification: DEAE-cellulose 52 column and Sephadex G-100 column Se detection: AAS Structure characterization: FT-IR; HPGPC; GC; HPAEC; AFM	Liu et al. (2013)
SeLEP-1a	*Lachnum* YM38	NA-SS	206.99	4.00×10^4	Man, Glc, and Gal (78.4:11.2:9.2)	Se-O-C (666 cm^{-1}) Se = O (868 cm^{-1})	Both α-glycosidic linkage and β-glycosidic linkage	Se detection: AFS Structure characterization: HPGPC; IC; GC-MS; AFM; FT-IR; NMR; SEM	He et al. (2022)
sCPA	Chinese chestnut (*Castanea mollissima*)	NA-SS	573.9	/	Glucose	Se-O-C (636 cm^{-1}) Selenylation modification of C-1, C-2, C-3 and C-4 position in sCPA	Linear 1,6-α-$_D$-glucan	Purification: Q Sepharose Fast Flow anion exchange column and Sephacryl S-400 chromatography column Se detection: ICP-OES Structure characterization: HPGPC; HPLC; FT-IR	H. Li et al. (2017)

(Continues)

TABLE 2 (Continued)

SePS	Study objects	Se source	Se content in SePS (μg/g)	Mw (Da)	Monosaccharide composition and molecular ratio	Se bond and wavelength (cm^{-1})	Glycosidic linkage or conformation	Analysis method	Reference
Se-GUP	*Glycyrrhiza uralensis*	NA-SS	1339	0.58 x 10^4	/	O-Se-O (956.32 cm^{-1})	/	Purification: Sephadex G-100 column Se detection: ICP-OES Structure characterization: FT-IR	Araujo et al. (2021) and Lian et al. (2018)
Se-ASP	*Artemisia sphaerocephala*	$SeOCl_2$	22,400	7.35 x 10^4	Ara, Xyl, Man, Glc, and Gal (1:4.21:45.90:9.74:11.43)	FT-IR: C-O-Se (844.36 cm^{-1}) Se = O (1064.09 cm^{-1}); Raman spectra: C-O-Se (847.73 cm^{-1}) Se = O (1034.79 cm^{-1}) Selenylation occur at C-6 position in the form of Se^{4+}.	/	Se detection: AFS Structure characterization: FT-IR; Raman spectroscopy; XPS; NMR; AFM; SEC-MALL-OR; MB	S. Zhu et al. (2020)
GPSs	Garlic	NA-SS; GA-SA; GA-SS; $SeOCl_2$	29,400 26,300 10,500 9200	/	/	C-O-Se (669.18 cm^{-1}) Se = O (854.28 cm^{-1})	/	Purification: DEAE-cellulose 52 column Se detection: AFS Structure characterization: FT-IR	Gao et al. (2016)
Se-SWP	Sweet potato	NA-SS	12,740	/	/	/	/	Se detection: AFS	Yuan et al. (2017)
SemCVP-1S	*Catathelasma ventricosum*	NA-SS	1180 - 1860	/	Glc, Gal and Fuc (87.6%,10.4%, and 1.2%)	C-O-Se (609 cm^{-1}) Selenylation at C-6	1, 3-α-$_L$-Gal*p* or α-$_D$-Fuc*p*	Purification: DEAE-cellulose 52 column and Sephadex G-100 column Se detection: ICP-MS Structure characterization: HPGPC; GC; GC-MS; FT-IR; NMR; Congo red test	Y. Liu et al. (2017)
Se-RAPS-2	Alfalfa root	NA-SS	320	/	/	C-O-Se (925 cm^{-1}) Se = O (840 cm^{-1}) -$OSeO_2H$ group mostly substitutes at O-6 of OH group in the C-6 positions,	1, 3-α glycosidic linkage	Purification: DEAE-cellulose 52 column and Sephadex G-200 column Se detection: AFS Structure characterization: HPGPC; UV; FT-IR; NMR; HPLC	Gao et al. (2020)

(Continues)

TABLE 2 (Continued)

SePS	Study objects	Se source	Se content in SePS (μg/g)	Mw (Da)	Monosaccharide composition and molecular ratio	Se bond and wavelength (cm^{-1})	Glycosidic linkage or conformation	Analysis method	Reference
Se-SCP	Sweet corncob	NA-SS	/	9.02×10^4	Man, Gal, GluA, Ara, Glu, Fuc, Rha, GalA, and Xyl.	FT-IR: Se = O (726 cm^{-1}); Raman spectra: Se = O (near 732 and 861 cm^{-1})	/	Structure characterization: Wang et al. (2022) SEC–MALLS; GC-MS; IR; Raman spectroscopy; XPS; NMR; SEM; AFM	

Abbreviations: Mw, molecular weight; Ara, arabinose; Frc, fructose; Fuc, fucose; Gal, galactose; GalA, galacturonic acid; Glc, glucose; GlcA, glucuronic acid; GlcNAc, glucosamine; Man, mannose; Rha, rhamnose; Rib, ribose; Xyl, xylose. AAS, atomic absorption spectroscopy; AFM, atomic force microscopy; AFS, atomic fluorescence spectrometry; DLS, dynamic light scattering; DSC, differential scanning calorimetry; FT-IR, Fourier transform infrared spectrum; GC, gas chromatography; GC-MS, gas chromatography-mass spectra; GPC, gel permeation chromatography; HPAEC, high performance anion-exchange chromatography; HPLC, high-performance liquid chromatography; RP HPLC, reverse phase high-performance liquid chromatography; HPGPC, high-performance gel permeation chromatography; HPSEC-MALI-RI, high-performance size exclusion chromatograph coupled with multi-angle laser light scattering photometer and a refractive index detector; SEC-MALLS, size exclusion chromatograph coupled with multi-angle laser light scattering analyzer; SEC-MALL-OR, size exclusion chromatograph coupled with multi-angle laser light scattering photometer and Optilab refractometer; IC, ion chromatography; ICP-AES, inductively coupled plasma atomic emission spectrometry; ICP-MS, inductively coupled plasma mass spectrophotometer; ICP-OES, inductively coupled plasma optical emission spectrometry; MB, methylene blue spectrophotometric analysis; NMR, nuclear magnetic resonance; SEM, scanning electron microscopy; TEM, transmission electron microscopy; TGA, thermal analysis; UV, ultraviolet-visible spectroscopy; XAS, x-ray absorption spectroscopy; EXAFS, extend x-ray absorption fine structure; NA-SS, nitric acid-sodium selenite (HNO_3-Na_2SeO_3); GA-SA, glacial acetic acid-selenous acid; GA-SS, glacial acetic acid-sodium selenite.

radicata (Gao et al., 2018), as well as from tea leaves (J. Zhu et al., 2020; Zhu et al., 2019). To obtain the enriched SePS, the growth medium or soil is fortified with inorganic Se by the addition of Na_2SeO_3 or by spraying with Se fertilizer containing Na_2SeO_3. The inorganic Se is absorbed and transformed into SePS via the transport, anabolic, and biosynthetic mechanisms of fungi, algae, and plants, which accumulate and transform the Se into organic Se compounds such as SePS.

The ability to accumulate inorganic Se and its biotransformation into SePS varies among fungi, algae, and plants. Generally, the ability of fungi to convert inorganic Se to SePS is higher than that of algae and plants (Table 2). In the study of Zhu et al. (2019), SePS from natural and enriched Se-enriched green tea were obtained and compared. Enriched SePS was obtained from green tea by spraying Na_2SeO_3 solution on the foliage of the green tea leaves for its assimilation into the leaves. It was evidenced that Se content in the enriched SePS from tea is higher than that of the natural SePS obtained from tea grows in the natural environment. Importantly, it highlights the fact that distinct Se-enrichment methods impact the MW of the SePS, vis-a-vis enriched versus natural SePS. Zhu et al. (2019) reported the isolation of four distinct groups of enriched SePS from tea with average MW of 0.29, 5.42, 86.93, and 2412 kDa, while the natural SePS from the same tea variety was also found to consist of four distinct groups but they differ in their average MW of 1.30, 4.72, 19.25, and 1024 kDa. Se enrichment in growth conditions impacted SePS biosynthesis by tea in favor of producing higher MW SePS.

Selenopolysaccharides obtained from artificial or natural Se-enriched plants are different in Se content and molecular weight. The different enrichment methods can also result in differences in monosaccharide composition, type of glycosidic bond, conformation of the molecule, degree of cross-linking, modification in the structure, etc., which are illustrated in Section 2.5. The biological activities of SePS may vary due to the above difference and details can be found in Section 2.6.

2.4.2 | Extraction and purification of selenopolysaccharide

There are several methods reported for the extraction and purification of SePS from plants, fungi, and algae, and the principal consideration is to select conditions that would maintain the intrinsic properties of the SePS throughout the whole process to maintain its bioactivity.

Most of the polysaccharides in plants, fungi, and algae are located within the cell wall as cell wall polysaccharides. Therefore, the first step in the extraction of these materials

is grinding to facilitate the release of cell wall polysaccharides. In addition to conventional physical grinding methods, ultrasonic gas flow crushing technology has been applied to rupture the cell walls and similarly applied to fungal spores, thereby greatly improving the efficiency of polysaccharide extraction from them. As the cell walls are extensively enveloped by lipids of the cell membrane, the removal of lipids as well as lipophilic impurities needs to be conducted after mechanical grinding. Reflux with 85%–95% ethanol for 6–8 h is commonly applied for the removal of lipid and/or lipophilic impurities. The residual material can then be utilized for polysaccharide extraction.

Considering the variations in the physical and chemical characteristics of diverse polysaccharides (specifically SePS), the selection of an extraction method should be tailored to the structure and solubility of the desired compounds. There are numerous methods of polysaccharide extraction with three methods being usually applied, which are: (i) hot water extraction, (ii) dilute alkali–water solution extraction, and (iii) enzymolysis. The optimum extraction time, temperature, enzyme type and dosage, and alkali concentration are varied for SePS from different sources. Hot water extraction is the most widely used method of SePS extraction as these polysaccharides have high solubility and stability in hot water. The usual practice is to perform the extraction at 60–100°C for 2–6 h, using a ratio of solid to liquid at 1:8–1:20 w/v, and the extraction is repeated once or twice (Y. J. Zhu et al., 2020; Wang et al., 2013; Zhu et al., 2019). Nevertheless, hot water extraction is characterized by a lack of efficiency and is time-consuming, and potential hydrolysis of the SePS due to heating temperature must be considered. It also frequently necessitates supplementation with additional extraction methods to enhance the overall extraction process, and the selection of appropriate factors for different substances becomes imperative. Alkali–water extraction method targets the solubilization of acidic polysaccharides due to the maintenance of surface charge in these polysaccharides in alkali pH. Sodium hydroxide solution or sodium carbonate at 5%–15% (w:w) is usually employed to extract the acidic polysaccharides, and the extraction temperature is kept below 10°C to limit alkaline-driven degradation of glycosidic linkages of the polysaccharide. In practice, a combination of hot water extraction followed by dilute alkali extraction of the residue is usually applied to extract SePS (Shi, 2016). Cellulase, pectinase, papain, or a combination of these enzymes are used for polysaccharide extraction in the enzymolysis method, to break down cellulose, pectin, and proteins, respectively. The enzyme treatment releases the non-cellulosic and non-pectin polysaccharides from the cell wall and matrix in improving efficiency for the SePS extraction. Zhao et al. (2022), for example, used a mixture of cellulase, pectinase, and papain with a weight ratio of 2:1:1 and at a concentration of 14% (w:w) to extract SePS from tea leaves at a temperature of 50°C for 90 min. In addition to these three methods, other extraction methods such as microwave (Liu et al., 2018), high pressure (Gu et al., 2020), ultrasound, and pulsed electric fields (Gao et al., 2022) as assistant techniques to improve the extraction efficiency of SePS have been applied in some research. Depending on the source of the biological material from which polysaccharides are derived, it is essential to consider extraction conditions based on the distinct cell wall structures of plants, fungi, and bacteria. While polysaccharides generally exhibit solubility in water and insolubility in organic solvents, water serves as the most common extraction medium. This characteristic makes water the primary solvent in acid or alkali extraction, as well as in the enzymolysis method.

After the extraction process, the polysaccharides are purified to remove monosaccharides, amino acids, proteins, phenolics, and other organic contaminants. To date, all SePSs behave as polar polysaccharides with high solubility in water and insoluble in ethanol solution (Huang et al., 2020). Thus, following the extraction, a three- or fourfold volume of ethanol is added to the water extract and kept overnight at 4°C to induce precipitation of the SePS. Subsequently, a series of steps to remove impurities in the ethanol-precipitated SePSs are often conducted, which mainly involve deproteinization and decolorization. Protein removal can be achieved with a Sevag (n-butanol:chloroform, 1:5, v/v), hydrochloric acid, or trichloroacetic acid (TCA) solution. Sevag solution treatment is relatively mild and relies on proteins denaturing in chloroform leading to their precipitation, thus most often applied to deproteinize polysaccharide extract while maintaining polysaccharide bioactivity in the published literature. TCA (5%–30%, w/w) precipitation of proteins is highly efficient but a much harsher chemical condition in removing protein from a polysaccharide extract. For TCA, the SePS extract needs to be precooled in an ice bath owing to the strong acidity of the TCA solution that may cause partial polysaccharide degradation, and the mixture placed at 4°C for 4 h followed by centrifugation to obtain a protein-free polysaccharide solution. Among the three deproteinization methods, the hydrochloric acid method has the advantage of high efficiency, followed by the TCA method and Sevag methods. Unlike the hydrochloric acid and TCA methods, which have the advantages of simple operation and stable results, the Sevag method requires longer deproteinization time to achieve the desired effect. However, the Sevag method has the significant advantages of lower polysaccharide loss and much milder extraction conditions that preserve the polysaccharide structure. For plant materials such as tea, the water-extracted solution

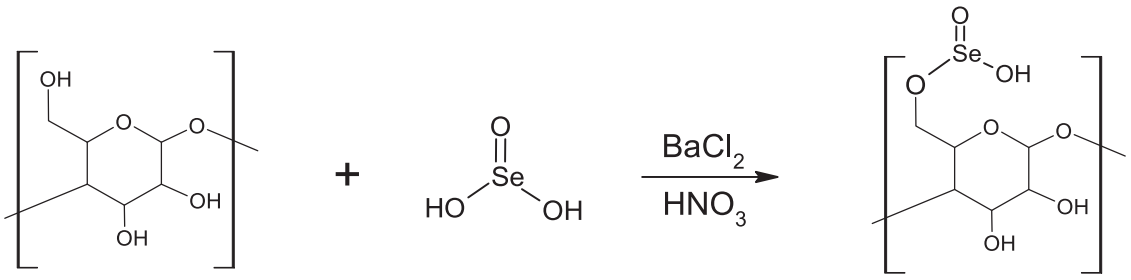

FIGURE 3 Proposed structure of Se-containing polysaccharide generated by the reaction of polysaccharide with nitric acid-sodium selenite. Selenylation with -$HSeO_3$ group occurs at C-6 (Wei et al., 2019).

is often dark in color due to the co-extraction of leave colored pigments such as anthoxanthin and anthocyanins and the tea polyphenol advance oxidation products such as theaflavin and theabrownin (Chaplin, 2006). Hydrogen peroxide can be used to decolorize the crude polysaccharide solution by breaking down the colored compounds and the crude extracted polysaccharides need to be purified to obtain purer and more homogeneous polysaccharide fractions. For polysaccharide purification, column chromatography is most widely applied, which has the advantages of high purity of the elute, high efficiency, and ease of operation. Anion exchange column chromatography is also employed; the most common method uses anion exchangers such as DEAE-cellulose, DEAE-Sepharose, and DEAE-Sephadex that are suitable for purifying various acidic or neutral polysaccharides and mucopolysaccharides (Chaplin, 2006; Shi, 2016). Other methods that can be used to purify the polysaccharides included: (i) graded precipitation, based on differences in solubility in alcohol and ketone solutions; (ii) salting-out method, based on differences in solubility in salts such as NaCl, KCl, and $(NH_4)_2SO_4$; (iii) metal coordinator method, based on differences in forming precipitate with metal ions; (iv) quaternary ammonium salt precipitation method; (v) ultracentrifugation method; (vi) ultrafiltration method; and (vii) preparative zone electrophoresis method (Shi, 2016).

2.4.3 | Chemically synthesized selenopolysaccharide

To improve the biological or physiochemical properties of native polysaccharides, the chemical selenylation method may be applied. Synthetic SePS can also be obtained by chemical synthesis methods using PS, and these included: (i) selenylation reaction with H_2SeO_3 reagents (Figures 3 and 4), (ii) addition of Se using chemically active selenium oxychloride ($SeOCl_2$) (Figure 5), and (iii) introducing Se by chemical attachment of functional groups containing Se (Yang et al., 2021).

There are four selenylation systems documented, which are nitric acid–sodium selenite (HNO_3-Na_2SeO_3), nitric acid–selenous acid (HNO_3-H_2SeO_3), acetic acid–sodium selenite (CH_3COOH-Na_2SeO_3), and acetic acid–selenous acid (CH_3COOH-H_2SeO_3). As shown in Table 2, the Se content in these selenylation-obtained synthetic SePS can be significantly higher than that of natural or enriched SePS.

Yuan et al. (2017) reported SePS with a very high Se content of 12.74 mg/g using polysaccharides extracted from sweet potato as the substrate (precursor) and $BaCl_2$ as the catalyst in the HNO_3-Na_2SeO_3 method. It has been shown that Ba^{2+} can improve selenylation efficiency of polysaccharides (J. Wang et al., 2012). Similarly, Lian et al. (2018) synthesized SePS with a Se content of 1.339 mg/g using polysaccharides from *Glycyrrhiza uralensis*, Zhu, Yu et al. (2020) synthesized SePS with a Se content of 2.12 μg/g using polysaccharides from tea, Gao et al. (2020) synthesized SePS with a Se content of 320 μg/g using polysaccharides from alfalfa roots, and He et al. (2022) synthesized SePS with a Se content of 206.99 μg/g using polysaccharides isolated from *Lachnum*, all by the selenylation reaction method.

The second chemical method uses $SeOCl_2$ which is a strong acylation agent targeting the hydroxyl groups of polysaccharides. SePS with a Se content of 22.4 mg/g can be synthesized by this method using polysaccharide from *Artemisia sphaerocephala* (Zhu, Hu et al. (2020). In the study of Gao et al. (2016), SePS were synthesized using different selenylation systems based on polysaccharides extracted from garlic. Selenopolysaccharides obtained with HNO_3-Na_2SeO_3 had the highest Se content at 29.4 mg/g, followed by those with CH_3COOH-H_2SeO_3, CH_3COOH-Na_2SeO_3, and $SeOCl_2$ with a Se content of 26.3, 10.5, and 9.2 mg/g, respectively. Additionally, the weight ratio of Na_2SeO_3 to polysaccharide and the effect of reaction temperature and time were also evaluated, which showed a ratio at 0.8:1, and reacting at 70°C for 10 h produced optimal selenylation of the polysaccharide. A host of other studies have also documented the synthesis of SePS by the HNO3-Na_2SeO_3 selenylation method using

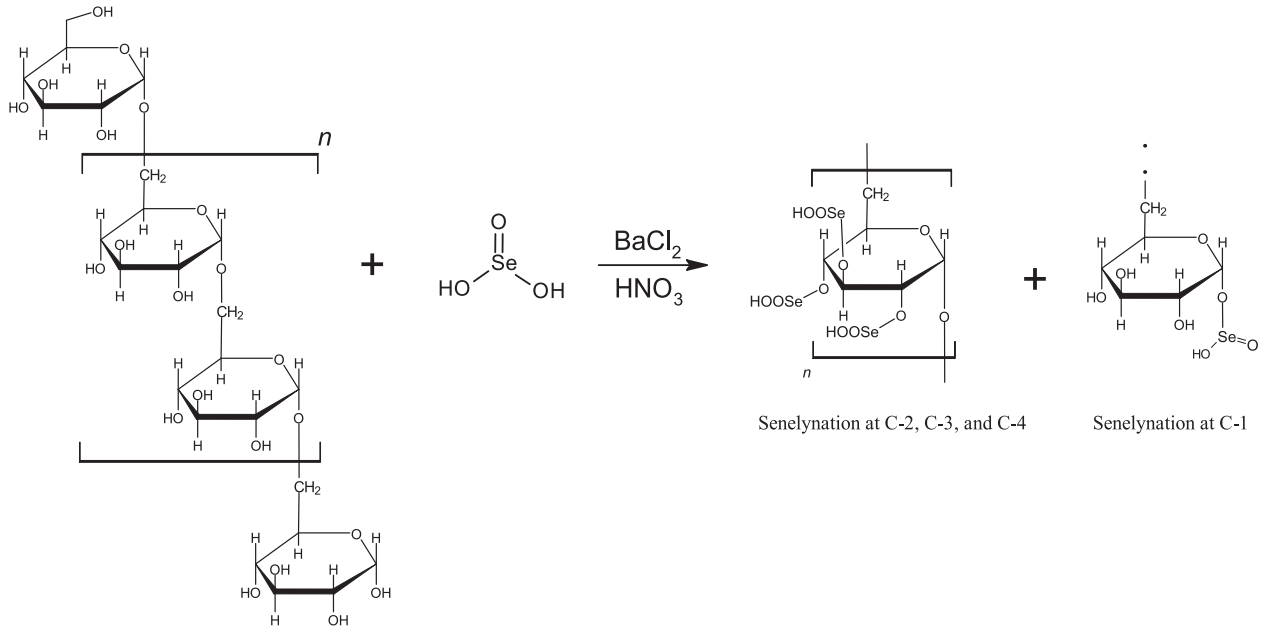

FIGURE 4 Proposed structure of Se-containing polysaccharide generated by the nitric acid–sodium selenite (HNO_3-Na_2SeO_3) method with 1-6-linked polysaccharide. Selenylation with -$HSeO_3$ group can occur at C-2, C-3, and C-4 positions and at C-1 position of the reducing sugar (H. Li et al., 2017).

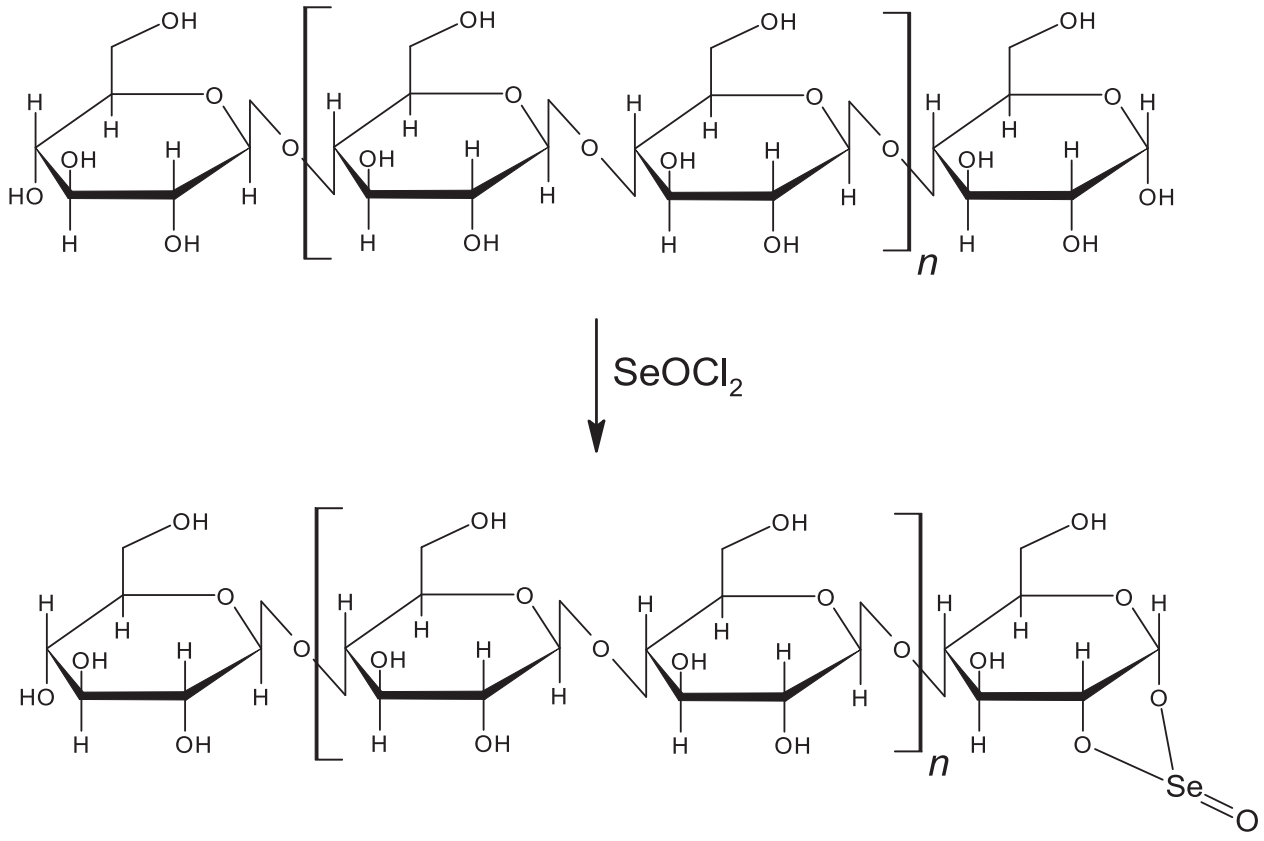

FIGURE 5 Proposed structure of Se-containing polysaccharide generated by the selenium oxychloride ($SeOCl_2$) method with 1-4-linked polysaccharide. Selenylation with -Se = O group can occur with both C-1 and C-2 in the reducing sugar forming a 5-atom ring structure (Górska et al., 2021; Huang et al., 2020; S. Zhu et al., 2020).

partially purified polysaccharides from a variety of sources. Selenylated SePS using polysaccharide from sweet corncob was confirmed by x-ray photoelectron spectroscopy (XPS) that shows the added Se specie as the selenite group (-O-Se[O]-OH) (Z. Wang, Wang, Xiu, & Ma, 2022). Selenylated SePS using polysaccharide from Chinese chestnut has a Se content of 573.9 μg/g (H. Li et al., 2017), while selenylated SePS using polysaccharide from the mycelia of *C. ventricosum* has Se content ranges from 1.18 to 1.86 mg/g (Y. Liu et al., 2017).

Chemically synthesized SePS tends to have a higher Se content than that of natural and enriched SePS. The evaluation of the selenylation magnitude is determined by the degree of substitution (DS), defined as the number of Se groups per monomer unit, and the maximum DS is contingent upon both the polysaccharide's structure and the nature of the reaction. The SePS obtained through these methods exhibits biological activity, which will be discussed in Section 2.6.

2.5 | Structure and characterization of selenopolysaccharide

The biological function of the macromolecule has a close relationship to its chemical structure; therefore, it is necessary to determine the structure of the SePS to reveal this relationship. Generally, structural characterization of the SePS is performed at increasing levels of detail, starting with its Se content, monosaccharide composition and glycosidic linkages, Se forms, binding site on the sugar structure, and the polysaccharide higher-order structure and micromorphology.

2.5.1 | Characterization of selenopolysaccharide

The Se content of the SePS can be determined by atomic fluorescence spectrophotometry (Gu et al., 2020; Zhao et al., 2022), atomic absorption spectrometry (AAS) (Gao et al., 2018; Ma et al., 2022), inductively coupled plasma mass spectrometry (Dong, Xiao et al., 2021; Zhou et al., 2020), inductively coupled plasma optical emission spectrometer (Lian et al., 2018), or inductively coupled plasma atomic emission spectrometry (Zhang et al., 2020). The carbohydrate content and protein content can be quantified by the phenol–sulfuric acid and the Bradford method, respectively. The MW of the SePS is often determined by high-performance gel permeation chromatography (He et al., 2022; Liu et al., 2022; Zhang et al., 2021). The monosaccharide composition of the SePS is usually identified, after their release from the polysaccharide, by gas chromatography (GC), HPLC, and MS (Dong, Xiao et al., 2021; Liu et al., 2022; Xiang et al., 2022). The chemical groups and glycosidic linkage configurations can be identified by FT-IR, laser Raman spectroscopy, or NMR (Xiang et al., 2022; Zhao et al., 2022).

Scanning electron microscope, atomic force microscope, and transmission electron microscope can be applied to observe the micromorphology of SePS (Gu et al., 2020; He et al., 2022; Zhang et al., 2021). The secondary structure of SePS in solution can be detected by circular dichroism spectroscopy (Duan et al., 2022). Additionally, other methods such as the Congo red test can be used to detect the presence of triple-helix structure in SePS, since Congo red can form complexes with polysaccharides in a triple-helix conformation and result in a red shift in the absorption maxima wavelength (λ_{max}) (Gu et al., 2020; J. Zhu et al., 2020); Zhang et al., 2021. It has been demonstrated that the triple-helix structure of polysaccharides is related to certain biological activities (F. Liu et al., 2017). Iodine reagent (I_2-KI, 0.02% I_2, 0.2% KI) can be used to determine the relative amount of side chains of polysaccharides by observing the intensity of the 565-nm wavelength absorption peak (J. Zhu et al., 2020). This is a relatively easy method for monitoring the integrity of the SePS during the purification process as changes would indicate alteration of the original structure (Wang et al., 2023). The size distribution of SePSs can be analyzed by dynamic light scattering (Zhang et al., 2021). XPS can provide qualitative information about different surface elements on samples (S. Zhu et al., 2020), while x-ray absorption spectroscopy can provide information about the oxidation state of an absorbing atom (Malinowska et al., 2018).

Besides, high-performance anion-exchange chromatography can be used to quantify uronic acid composition in SePS (Liu et al., 2013), and size exclusion chromatograph can be applied to access the size and conformation of the SePS (S. Zhu et al., 2020).

2.5.2 | Structure and selenium forms of natural and enriched selenopolysaccharide

The structural diversity and complexity of natural and enriched SePSs lie in the multiple ways in which Se can form bond(s) with the atomic entity of the sugars. At present, these Se forms have been identified to include Se-O-C, O-Se-O, Se = O, and Se-H groups, all occurring as part of the sugar structure. Monosaccharides containing Se atom may alter the polysaccharide structure from which the monosaccharides form the polymer backbone. Additional complexity arises from the ratio of the monosaccharide that varies between "natural" and "enriched" growth conditions in producing the natural and enriched SePSs, respectively.

The main chain of natural and enriched SePS isolated from tea to date are composed of 1−3, 1−4, or 1−6 glycosidic linked α- or β-$_D$-glucopyranose units, and with β-$_D$-Man$_p$(1-3), β-$_D$-Man$_p$(1-6), α-$_D$-Gal$_p$(1-3), α-$_D$-Gal$_p$(1-6), β-$_D$-Glc$_p$(1-4), β-$_D$-Glc$_p$(1-4), and β-$_D$-Glc$_p$(1-6) branched sugars linked to the main chain. Zhao et al. (2022) isolated natural SePS (SeTPS-1, −2, and −3) from tea grown in high Se soil region and showed that the sugars consisted of mannose, glucose, galactose, xylose, arabinose, and glucuronic acid in different ratios and that all the sugars are in the pyranose configuration and β-glycosidic linkages (Table 2). Ultraviolet–visible spectroscopy and FT-IR analysis showed absorption peaks at 676, 799, and 1050 cm^{-1}, which were attributed to Se-O-C stretching vibration, Se = O stretching vibration, and O-Se-O bond of Se ester, respectively.

Gu et al. (2020) extracted two natural SePSs (SeTPS-1, −2) from tea, again grown in a high Se soil region, in which SeTPS-1 is composed of glucose and galactose with a molar ratio of 80.1:2.3, while SeTPS-2 is composed of arabinose, glucose, galactose, and galacturonic acid at a molar ratio of 2.04:48.83:3.21:1.30. The glycosidic linkage in both SeTPS-1 and SeTPS-2 is in the α-glycosidic form, and both SePSs adopted a random coil conformation. The FT-IR absorption peaks observed at 1025 and 763 cm^{-1} were assigned to the O-Se-O and Se = O groupings.

Similarly, J. Zhu et al. (2020) isolated a natural SePS from tea (ASe-TPS1), which is also a heteropolysaccharide rich in glucose and also contains rhamnose, arabinose, galactose, glucose, xylose, mannose, fructose, and galacturonic acid in a molar ratio of 0.16:0.25:0.76:1.00:0.05:0.10:0.12:0.31. The FT-IR absorption peaks at 611, 669, and 1080 cm-1 were assigned to Se-O-C tensile vibration, Se-H stretching vibration, and O-Se-O asymmetric tension.

It was speculated that Se may exist in the form of -SeH on the branch sugars of the polysaccharide, owing to the bathochromic shift of two absorption peaks on the pyran ring, from 1133 and 1112 cm^{-1} to 1151 and 1122 cm^{-1}, respectively (J. Zhu et al., 2020). Branching introduces steric hindrance and changes in the local environment around the chromophore, which affects the distribution of electron density and alters the energy levels of electronic transitions, which leads to the absorption peaks shifting to longer wavelengths. Raman spectra analysis showed the absorption peaks at 742 and 664 cm^{-1} that could indicate the presence of Se = O and Se-OH groups in the polysaccharide, and the absorption peaks around 791 and 632 cm^{-1} from Raman spectral were assigned to the C-O-Se group. Based on the detection of Se = O, Se-OH, and C-O-Se groups in the spectral analysis, selenol-carrageenan (-OSe[O]OH group bound to sugar) was speculated to also exist in the polysaccharide. NMR analysis revealed that most of the Se in ASe-TPS1 replaced the O atom in the C-1 of the branch sugars of the polysaccharide and exists in the form of -SeH, and also suggested the possibility of Se at C-3 of the sugars, due to the absence of chemical shift signal at the C-6 position and the chemical shift to the low field at the C-3 position. However, it demonstrated that for Se in the chemically synthesized tea polysaccharides (CSe-TPS1), Se replaces the hydroxyl group of the C-6 position in the form of selenyl ether.

Zhu et al. (2019) isolated natural SePSs (NSe-TPS2) from tea where the tea was cultivated in a Se-enriched area (Enshi, Hubei Province, China) and enriched SePSs (ASe-TPS2) where the tea leaves were sprayed with a selenium fertilizer (Na_2SeO_3 solution) during cultivation. Significant differences were found between these two SePS sources. NSe-TPS2 has a Se content of 0.44 μg/g, an MW of 2.44×10^5 Da, and is composed of fucose, rhamnose, arabinose, galactose, glucose, glucuronic acid, and galacturonic acid. ASe-TPS2, on the other hand, has a higher Se content of 0.75 μg/g and MW of 6.73×10^3 Da and is composed of rhamnose, arabinose, glucose, xylose, and galactose. The structure of NSe-TPS2 was mainly composed of 1,4-β-$_D$-Glc*p* and 1,4-α-$_D$-Gal*p*A, and the branches predominantly consisted of 1,2-β-$_L$-Ara*f*, 1,3-α-$_D$-Gal*p*, and 1,2-β-$_L$-Rha*p*, with non-reducing Glc*p* or Gal*p* residues ends. However, the structure of ASe-TPS2 differs mainly composed of 1,3-β-$_D$-Glc*p*, 1,4-α-$_D$-Gal*p*A, 1,4-Glc*p*, 1,2-α-$_L$-Rha*p*, and with Ara*f* and Xyl*p* the non-reducing ends. Therefore, Se fortification during tea plant growth can produce a distinct SePS structure.

Besides tea, SePS was also isolated from weeds and fruit. Xiang et al. (2022) isolated two natural SePSs (Se-PPS1 and Se-PPS3) from the weed, pennycress (*T. arvense* L.), which have 1,6-β-$_D$-Gal*p* and terminal non-reducing α-$_D$-Glc*p* sugars and their configurations were determined by GC-MS and NMR. Se-PPS1 was found to compose of glucose, galactose, and arabinose at a ratio of 0.95:0.03:0.02, while Se-PPS3 was composed of glucuronic acid, rhamnose, galacturonic acid, glucose, galactose, xylose, and arabinose at a ratio of 0.17:0.03:0.08:0.31:0.22:0.06:0.13. FT-IR showed that the two SePSs had absorption spectra typical of polysaccharides and spectral characteristics of the Se groups, O-Se-O and Se = O. Liu et al. (2022) isolated natural SePSs (Se-RLFP-1 and Se-RLFP-2) extracted from the fruit of a Chinese herb, Michx (*R. laevigata*) and showed that Se-RLFP-1 was composed of 1,3-glycosidic linked rhamnose, xylose, and glucose with a molecular ratio of 0.12:0.51:0.39, while Se-RLFP-2 contain the same sugars but with a different molecular ratio of 0.39:0.44:0.17. The Se-O-C group in Se-RLFP-1 and Se-RLFP-2 was identified by FT-IR based on the 620.98 and 617.12 cm^{-1} absorption peaks, while the Se = O group was based on the absorption peaks at 761.76 and 760.89 cm^{-1}, respectively.

There were also successful isolations of enriched SePSs from fungi. Zhang et al. (2021) isolated an enriched SePS (Se-POP-21) from *P. ostreatus* cultivated in Se-fortified compost irrigated with 90 ppm Na_2SeO_3 solution. Se-POP21 was found to be composed of mannose, glucose, galactose, and arabinose in a molecular ratio of 18.01:2.40:26.15:7.34. Characteristic absorption peaks of Se-O-C and Se = O were also observed by FT-IR, at 654 and 756 cm^{-1}, respectively. Zhang et al. (2022) also isolated an enriched SePS (Se-POP3) from *P. ostreatus* where the mushroom was cultivated in Se-fortified compost irrigated with 90 ppm Na_2SeO_3 solution. While Se-POP3 was also found to be composed of mannose, glucose, and galactose with a molecular ratio of 1.7:49.6:2.4, arabinose was notably absent. The sugars in Se-POP3 were linked by both α- and β-glycosidic linkages, and characteristic FT-IR absorption peaks of C-O-Se and Se = O were similarly observed at 660 and 758 cm^{-1}, respectively. By contrast, Ma et al. (2022) also isolated an enriched SePS from *P. ostreatus* (Se-POP1) fortified with Na_2SeO_3 solution. Se-POP1 had significantly different IR absorption peaks of the Se bonds compared to Se-POP-21 and Se-POS3, where Se-POP1 exhibited two FT-IR absorption peaks at 941 and 1048 cm^{-1} attributed to C-O-Se and Se = O stretching vibrations, respectively. Selenium in the enriched SePS isolated from *G. frondosa* existed in Se-O-C, O-Se-O, and Se = O bond forms, with characteristic FR-IR absorption peaks at 667.9, 1024.5, and 759.9 cm^{-1}, respectively, and it was composed of mannose, glucose, and galactose (Q. Li et al., 2017). The existence of Se bonds in O-Se-O and Se = O forms with absorption peaks at 977.25 and 891.43 cm^{-1} was also identified in enriched SePS from *C. militaris* (Ren et al., 2020), and it was composed of mannose, ribose, glucose, galactose, arabinose, and glucuronic acid. Plus, Se bonds in O-Se-O, Se = O, and Se-H forms with absorption peaks at 919.87, 460, and 670 cm^{-1}, respectively, were also found in enriched SePS from *P. igniarius* by Luo et al. (2021). For the enriched SePS from *L. edodes* (Malinowska et al. (2018), except for the Se = O bond forms at the C-6 position in the polysaccharide, the most probable Se forms include the substitution of Se on oxygen (O) in the β-glucose acetal ring, and the incorporation of Se in the glycosidic linkage (Figure 2). All these enriched SePSs were obtained by cultivating the mushroom in compost fortified with Na_2SeO_3 solution. It is thus clear that, as with tea, enriched SePSs from mushrooms showed differences in the polysaccharide structure and Se forms, and that the level of Na_2SeO_3 fortification of the growth compost for the mushroom also affected these. Additionally, the structure characteristics of mushroom SePSs also appear to vary depending on the mushroom species.

Natural and artificial SePSs show different characteristics in structure, which also needs to take into account the influence of the food material/plant itself. In future studies, to further understand the nutritional value of SePS, more exploration of natural SePSs, artificial cultivation methods of Se-rich plants, and structural analysis of these polysaccharides are needed.

2.5.3 | Structure and selenium forms of synthetic selenopolysaccharide

The structure characteristics of chemically synthesized synthetic SePS not only differ from natural and enriched SePSs but also vary depending on the chemical selenylation methods employed. Chemical selenylation mostly occurs at C-6 of the sugar in the SePS, largely due to the C6-OH primary alcohol being more reactive and more physically accessible than other OH groups on the sugar.

Liu et al. (2013) prepared a synthetic SePS (SemCVP-1S) using polysaccharides extracted from *C. ventricosum*, and selenylation of the polysaccharide using the HNO_3-Na_2SeO_3 method. SemCVP-1S was found to be composed of 1,3-α-$_L$-Gal*p* or α-$_D$-Fuc*p*, while the FT-IR showed a new signal at 609 cm^{-1} that is not present in the original polysaccharide which the authors assigned to a Se-O-C stretching vibration. NMR spectra revealed that the selenylation substitution mostly occurred at C-6 of the sugars as the selenite -O-Se[O]OH group. Congo red tests indicated that the triple-helical structure of the original polysaccharide is absent in SemCVP-1Ss, possibly due to the presence of the seleno groups.

Chemically selenized alfalfa root polysaccharides (Se-RAPS-2) using HNO_3-Na_2SeO_3 showed two new absorption peaks in the FT-IR spectrum at 925 and 840 cm^{-1}, which were attributed to the C-O-Se stretching vibration and the Se = O asymmetric stretching indicating the incorporation of the selenol-group also in the form of -O-Se[O]OH (Gao et al., 2020). NMR analysis confirmed substitution in the C-6 position of the sugars. Similarly, chemical selenylation of *G. uralensis* polysaccharides HNO_3-Na_2SeO_3 obtained a SePS (Se-GUP) with an absorption peak at 956.32 cm^{-1} attributed to the O-Se-O group in the selenite group (Cheng et al., 2020; Lian et al., 2018).

It seems that chemical selenylation of polysaccharides with H_2SeO_3 favors the C-6 position of sugars in producing these synthetic SePSs (Figure 3); however, selenylation on the sugar C-1, C-2, C-3, and C-4 positions have also been reported (Figure 4). Synthetic SePS (sCPA) chemically synthesized with polysaccharides extracted from Chinese chestnut (*Castanea mollissima*) using HNO_3-Na_2SeO_3 showed a new FT-IR peak at 636 cm^{-1}, which was attributed to an asymmetrical Se-O-C stretching vibration (H. Li et al., 2017). However, the distortionless enhancement by polarization transfer (DEPT) (135°) spectrum of sCPA indicated that selenylation with selenite occurred at

C-1 (δ 100.1), C-2 (δ 75.0), C-3 (δ 73.9), and C-4 (δ 72.6) positions. As reported by the literature above, the non-selective selenylation polysaccharides are prone to happen at the C-6 position. However, owing to the 1,6-linked glucan structure of this polysaccharide, the C-6 position is not available for selenylation; hence, selenylation was directed to other -OH sites.

Enriched SePS and synthetic SePS differ not only in Se content but also in distinct Se structures and bonds. In addition to an enriched SePS (ASe-TPS1), which was obtained from biofortified tea leaves sprayed with sodium Na_2SeO_3 solution during growth, J. Zhu et al. (2020) also chemically synthesized a synthetic SePS from non-Se-containing polysaccharides from the same tea (CSe-TPS1) using HNO_3-Na_2SeO_3. Both ASe-TPS1 and CSe-TPS1 are acidic heteropolysaccharides with different Se content, monosaccharide composition, and molar ratio. These differences are expected since they are obtained by different means in which the Se status of the growing leaves affected the polysaccharide synthesis (biosynthetically vis-à-vis chemically). As indicated before, Se replaces the hydroxyl group at the C-1 and C-6 positions in ASe-TPS1 in the form of a Se-H bond on the branched sugar of the polysaccharide. By contrast, spectra analysis revealed that most of the Se in CSe-TPS1 is in the form of selenyl ether (Se-O-C at 611 cm^{-1} and O-Se-O at 1080 cm^{-1}) on the C-6 position of the sugars in the polysaccharide, that is, as a selenite group.

A synthetic SePS (Se-ASP) obtained by $SeClO_2$ selenylation method using polysaccharides isolated from *A. sphaerocephala* has the Se inserted as a selenite group on the C-6 position of the sugar, based on FT-IR absorption peaks at 844.36 and 1064.09 cm^{-1} from C-O-Se and Se = O chemical groups, respectively, and it has been further confirmed through XPS analysis that the Se 3d signal was in the Se^{4+} oxidation state indicating that Se existed in the selenite form (S. Zhu et al., 2020). However, Se insertion patterns other than as a selenite group can be obtained with the $SeClO_2$ method. It was found that when $SeClO_2$ reacts with polysaccharides, a seleno-group with a five-membered ring structure could be formed by adjacent hydroxyl groups in a homeotropic relationship (Figure 5). Therefore, the two cis-hydroxyl groups at C-1 and C-2 in the α-reducing sugar of the polysaccharides from *Astragalus* can generate five-membered Se-containing rings (Huang et al., 2020).

2.6 | Biological activities of selenopolysaccharide

The selenylation of polysaccharides not only alters their structural and chemical characteristics but can also create new or enhance existing activities. Besides antioxidant activity, SePSs also possess several biological activities that may arise from increasing cellular antioxidant defense. The biological activities of SePSs are listed in Table 3, and they included SePS effect on diabetes (He et al., 2022; Liu et al., 2013; Y. J. Zhu et al., 2020; Liu et al., 2017), tumor development (Cheng et al., 2018; Gao et al., 2020; S. Zhu et al., 2020; Zhang et al., 2022, 2021), DNA damage (Gu et al., 2020), as well as immunomodulation (Gao et al., 2016), intestinal barrier enhancement and gut microbiota regulation (Zhao et al., 2022), neuroprotection (Liu et al., 2022), and heavy metal detoxification (Zhou et al., 2020). Importantly, SePS shows significantly increased bioactivity when compared to the non-selenized polysaccharides from the same source. Selenium modification of polysaccharide structures through biotechnological or chemical means can induce substantial alteration in their biological activity, which involves the introduction of Se into the polysaccharide sugar entities modifying their primary and secondary structures.

2.6.1 | Selenopolysaccharide as a dietary source of selenium

The bioavailability of dietary Se ranges from 29% to 98% dependent on the sources and Se forms (Arshad et al., 2021; Lei et al., 2022). Inorganic Se compounds could probably be used as Se sources in dietary supplements due to their cost-effectiveness, for example, when added to animal feed (Liao et al., 2011). However, it is still a challenge for safe and effective supplementation of inorganic Se considering its low bioavailability, high cytotoxicity, and short retention time in the gastrointestinal tract. Numerous evidence indicate that organic Se is more bioavailable from foods and is more effective than inorganic Se in providing antioxidant protection to cells and tissues, thereby improving immune function and immunomodulation and providing anti-cancer and anti-inflammation effects (Feng et al., 2021; Gandin et al., 2018; Jiang et al., 2022, 2021; Rua et al., 2023). Organic Se such as selenoamino acids and selenoproteins have been well-studied, and they can be found in dietary suitable levels in some crops and vegetables cultivated in Se sufficient soil and can also be found in some animal products from animals with sufficient Se intakes. While selenocysteine, methylselenocysteine, and selenomethionine are well-established in biological systems with defined roles, selenoneine is a more recently discovered Se-containing amino acid found in certain aquatic organisms (El Hanafi et al., 2022; Yamashita & Yamashita, 2010; Yamashita et al., 2013), and its precise biological functions are still under investigation. Numerous studies have focused on finding other types of organic

TABLE 3 Biological activities of selenopolysaccharides.

SePS	Study objects	Se content in SePS (μg/g)	SePS concentration	Study model/method	Biological effects	Reference
SeTP	Tea	7.93 ± 0.14 (SeTPS-1); 5.59 ± 2.28 (SeTPS-2); 6.00 ± 2.93 (SeTPS-3)	250 mg/kg/day; 500 mg/kg/day; 750 mg/kg/day;	In vivo: DSS-induced colitis mice (C57BL/6 male mice [20 ± 2 g; 6-week])	Enhance intestinal barrier; regulate gut microbiota.	Zhao et al. (2022)
SeZYTP	Tea	2.14	25–200 μg/mL (cell study); 100, 200, and 400 μg/kg body weight per day (animal study)	In vitro: human osteosarcoma U-2 OS cells; In vivo: treatment on U-2 OS cancer xenograft model in BALB/c athymic mice for 28 days	Anti-tumor: suppress the proliferation of human osteosarcoma U-2 OS cells in a dose-dependent; and obvious tumor regression.	Y. Wang et al. (2013)
SeTPSs	Tea	0.97 (SeTPS1); 0.44 (SeTPS); 0.34 (SeTPS3)	25, 50, 100, 200, and 400 μg/ml	Antioxidant assays (DPPH, superoxide radicals scavenging assay)	Antioxidant	Wang et al. (2015)
SeTPS	Tea	2.76 ± 0.10	50–200 mg/kg body weight per day	In vivo: S180 cancer xenograft model in Kunming mice (oral administration of SeTPS for 13 days	Anti-tumor: inhibit the proliferation of sarcoma S-180 tumor cells in dose-dependent manner.	Cheng et al. (2018)
SeTPSs	Tea	23.50 (SeTPS-1); 13.47 (SeTPS-2)	0.2–1.2 mg/mL	Antioxidant assays (ABTS, hydroxyl radicals scavenging assay)	Antioxidant; DNA damage protective effect.	Gu et al. (2020)
ASe-TPS1 CSe-TPS1	Se-enriched; artificial Se-enriched tea	1.64 ± 0.48 (ASe-TPS1); 2.12 ± 0.24 (CSe-TPS1)	200, 400, 600, 800, and 1000 μg /mL	Alpha-glucosidase inhibitory activity assay	Anti-diabetic: dose-dependent inhibition against α-glucosidase.	J. Zhu et al. (2020)
Se-RLFPs	Michx fruits (*Rosa laevigata*)	16.49 ± 0.12 (Se-RLFP-1); 21.61±0.47 (Se-RLFP-2)	3.0–5.0 mg/mL	In vitro: ABTS; DPPH; FRAP; neuroprotective activity test on H_2O_2-induced SH-SY5Y cell damage model	Antioxidant; neuroprotective activity.	Liu et al. (2022)

(Continues)

TABLE 3 (Continued)

SePS	Study objects	Se content in SePS (μg/g)	SePS concentration	Study model/method	Biological effects	Reference
Se-PPSs	Pennycress (*Thlaspi arvense* L.)	13.56 ± 1.87 (Se-PPS1); 15.36 ± 2.30 (Se-PPS3)	20–40 μL	Antioxidant assays (DPPH, hydroxyl, and superoxide radicals scavenging assay)	Antioxidant	Xiang et al. (2022)
Se-L	*Lentinula edodes*	190	1, 10, and 100 μg/mL	In vitro: normal (HUVEC) and malignant (HeLa) cells	Antioxidant: Se-L showed stronger antioxidant activity, which was non-toxic and even enhanced cell viability.	Kaleta et al. (2019) and Malinowska et al. (2018)
Se-SPP	*Spirulina platensis*	14.12 ± 1.41	100 mg/kg body weight	In vitro: human liver cell line (HL-7702) and human embryonic kidney cell line (HEK293) In vivo: CdCl2-intoxicated rats, 30 healthy male Sprague Dawley (SD) rats (n = 6/group; age = 6 weeks; body weight ~180 g)	Cytoprotective role against Cd-induced toxicity.	Zhou et al. (2020)
Se-POP-3	*Pleurotus ostreatus*	25.9	0, 50, 100, 200, 400, 600 μg/mL	In vitro: eight human tumor cell lines (MGC-803 cells, HCT-116 cells, NCM460 cells. HepG2, MCF-7, SKOV3, HeLa, and PC-3) and three human normal cell lines (L02, MCF-10A, IOSE)	Anti-tumor (gastric cancer, colon cancer): Se-POP-3 could induce apoptosis and inhibit migration of these tumor cells.	Zhang et al. (2020) and Y. Zhang et al. (2022)
Se-POP-1	*Pleurotus ostreatus*	3.69	400 μg/mL	In vitro: H_2O_2-stimulated PC12 cell model	Antioxidant; anti-apoptosis.	Ma et al. (2022)

(Continues)

TABLE 3 (Continued)

SePS	Study objects	Se content in SePS (μg/g)	SePS concentration	Study model/method	Biological effects	Reference
Se-POP-21	*Pleurotus ostreatus*	5.31	0, 0.2, 0.4, 0.6, 0.8, 1.0, 1.2 mg/mL (antioxidant assays) 0, 50, 100, 200, 400, 600 μg/mL (cell study)	Antioxidant assay (DPPH, hydroxyl radical) In vitro: A549, SKOV3, HepG2 and MCF-7 cells	Antioxidant; antitumor (lung cancer, ovarian cancer, liver cancer, breast cancer): Se-POP-21 could decrease viability of A549, SKOV3, HepG2 and MCF-7 cells, induce apoptosis, and suppress metastasis of A549 cells.	Zhang et al. (2021)
SPMP-2a	*Pleurotus geesteranus*	/	100, 200, and 300 μg/mL	In vivo: hydrogen peroxide (H_2O_2)-induced oxidative damage in HaCaT cells	Antioxidant: alleviate oxidative damage by enhancing cellular antioxidant enzyme activities, reducing ROS levels, and promoting the expression of Bcl-2 protein, thereby reducing cell apoptosis and protecting HaCaT cells from H_2O_2-induced oxidative damage.	Sun et al. (2017)
PSeP	*Phellinus igniarius*	120.00	100, 200, 300, 400, and 600 μg/mL (cell study) 200, 400, and 600 mg/mL (animal study)	In vivo: hydrogen peroxide (H_2O_2)-induced oxidative damage in HaCaT cells In vivo: male Kunming mice (aging 4 weeks and weighting 20 ± 2 g)	Antioxidant: the administration of PSeP could reduce ROS level by enhancing the activities of GSH-Px.	Luo et al. (2021)
Se-GFP-22	*Grifola frondose*	8.37	0, 200, 400, 600, 800, 1000, 1500, and 2000 μg/mL	Antioxidant assay: DPPH	Antioxidant	Q. Li et al. (2017)
SPS	*Oudemansiella radicata*	127.1	200 and 400 mg/kg/day	In vivo: lipopolysaccharide-induced endotoxemic mice (Kunming strain mice, male, aging 8–10 weeks, body weight 18–22 g)	Antioxidant: enhance the activities of SOD, GSH-Px, CAT and T-AOC, suppress the MDA and LPO contents both in lung and kidney; anti-inflammatory: reduce MPO activities in lung.	Gao et al. (2018)

(Continues)

TABLE 3 (Continued)

SePS	Study objects	Se content in SePS (μg/g)	SePS concentration	Study model/method	Biological effects	Reference
PS-Se SLN-PS-Se	*Fomes fomentarius*	/	PS-Se (150 mg/kg b.w.); SLN-PS-Se (25 mg/kg b.w.)	In vivo: Wistar rats (200 ± 50 g)	Anti-hyperglycemic: the oral administration of PS-Se could reduce blood glucose level and HbA1c levels, and improve insulin secretion and body weight.	Keshavarz-Rezaei et al. (2022)
SeLEP-1a	*Lachnum* YM38	206.99	0.25, 0.75, 1, 3, and 5 mg/mL (assays) 0, 50, 100, 200, 400, 800 μg/mL (cell study)	In vitro: antioxidant assays (ABTS, DPPH, hydroxyl radical scavenging assays, reducing power assay). Alpha-glucosidase inhibitory activity assay and α-amylase inhibitory activity assay. Cell study: LO2 cells, Caco-2 cells, and HepG2 cells	Antioxidant; antidiabetic; non-cytotoxic to LO2 cells and Caco-2 cells within a certain concentration range.	He et al. (2022)
sCPA	Chinese chestnut (*Castanea mollissima*)	573.9	5, 10, 25, 50, or 100 μg/mL	In vitro: HeLa cells	Anti-tumor: the Se supplementation could suppress mitochondrial membrane potential and induce HeLa cells apoptosis. sCPA could also arrest HeLa cells in S phase, stimulate ROS generation, and activate caspase-3 activity in HeLa cells.	H. Li et al. (2017)
Se-GUP	*Glycyrrhiza uralensis*	1339			Antioxidant.	Araujo et al. (2021) and Lian et al. (2018)
Se-ASP	*Artemisia sphaerocephala*	22,400	0.63, 1.25, 5, 10, 20, 30, and 40 μg/mL	In vitro: HepG2 cells	Anti-tumor: high Se content could inhibit the proliferation of tumor cells.	S. Zhu et al. (2020)
GPSs	Garlic	29,400 26,300 10,500 9200	Twofold serially from 0.098 to 100 μg/mL	In vivo: adult non-vaccinated White Roman chickens (male)	Immune-enhancing activity.	Gao et al. (2016)

(Continues)

TABLE 3 (Continued)

SePS	Study objects	Se content in SePS (μg/g)	SePS concentration	Study model/method	Biological effects	Reference
Se-SWP	Sweet potato	12,740		Antioxidant assay (ABTS, DPPH) In vivo: SD rats (male, 320 ± 5 g, for anti-diabetic evaluation); Kunming mice (Female, aged 6 weeks, for anti-tumor evaluation)	Antioxidant; anti-diabetic; anti-tumor: inhibit tumor growth (>50%) and adjust immune factor (IL-2, TNF-α, and VEGF) levels.	Yuan et al. (2017)
SemCVP-1S	*Catathelasma ventricosum*	1180–1860	0.2 or 2.0 g/kg per day	In vivo: 48 streptozotocin-induced diabetic mice	Anti-diabetic: SemCVP-1S with medium Se content (1.54 mg/g) exhibited superior anti-hyperglycemic activity than that of SemCVP-1S with low (1.18 mg/g) and high (1.86 mg/g) Se content.	Y. Liu et al. (2017)
Se-RAPS-2	Alfalfa root	320	6.25, 12.50, 25.00, 50.00, and 100.00 μM	Antioxidant assay (ABTS, DPPH) *In* vitro: HepG-2 cells	Antioxidant; anti-tumor effect on HepG-2 cells in a dose-dependent manner.	Gao et al. (2020)
Se-SCP	Sweet corncob	/				Wang et al. (2022)
CSP-SeNP3	*Chaenomeles speciosa*	/	8.37 ± 0.97 μg/mL	In vitro: A549, MCF-7, and HepG2 cell models; In vivo: zebrafish model	Antitumor (breast cancer).	Zhou et al. (2022)

Abbreviations: ABTS, 2,2′-azino-bis-3-ethylbenzothiazoline-6-sulfonic acid scavenging assay; DPPH, 1,1-diphenyl-2-picrylhydrazyl radical scavenging assay; FRAP, ferric reducing antioxidant power assay; SOD, superoxide dismutase; GSH-Px, glutathione peroxidase; CAT, catalase; T-AOC, total antioxidant capacity; MDA, malondialdehyde; LPO, lactoperoxidase; MPO, myeloperoxidase; IL-2, interleukin-2; TNF-α, tumor necrosis factor alpha; VEGF, serum vascular endothelial growth factor; MGC-803 cells, human gastric cancer cells; HCT-16 cells, human colon cancer cells; NCM460 cells, normal human intestinal epithelial cells; HUVEC, human umbilical vein endothelial cells; HaCaT, human keratinocytes cells; SH-SY5Y, cells isolated from a bone marrow biopsy taken from a 4-year-old female with neuroblastoma; HeLa, an immortalized cell line, cervical adenocarcinoma; HepG2, human hepatoma carcinoma cells; MCF-7, human breast cancer cells; SKOV3, ovarian cancer cells; PC-3, human prostate cancer cells; LO2, human normal hepatocyte; MCF-10A, human mammary epithelial cell line; IOSE, simian virus 40-transformed human ovarian surface epithelial cells; A549, human lung cancer cells; Caco-2, human colorectal adenocarcinoma.

Se-containing compounds, aiming to enlarge the pool of organic Se available to the human diet in addition to the well-known selenoamino acids and selenoproteins. To date, studies continue to document the discovery of SePS from food materials as described above, indicating that SePS has the potential to be a suitable source of organic Se in the human diet to support body health.

The main antioxidant defense mechanism in cells involves antioxidant enzyme systems to eliminate superoxide anion, which is a by-product of mitochondria respiration, and other reactive oxygen species and free radicals and their buildup a major driver of cellular oxidative stress. The antioxidant enzymes in these systems included glutathione peroxidase (GSH-Px), superoxide dismutase (SOD), and catalase (CAT), and one of their main functions is to detoxify superoxide anion to hydrogen peroxide and, eventually, to water. They can also scavenge free radicals generated in cells, for example, those arising from lipid oxidations. GSH-Px is a selenoenzyme that requires Se for its biosynthesis, and an adequate supply of Se has been shown to enhance GSH-Px antioxidant activity in the body (Yang et al., 2021). There are other selenoenzymes besides GSH-Px and the non-enzyme selenoproteins that contain Se (Gencheva et al., 2022; Nicholson et al., 2022; Schweizer & Fabiano, 2022). Most are known to have important functions in the body. Besides inorganic Se, selenoamino acids, and selenoproteins from foods, SePSs can probably be an additional source of Se for the body. However, it is not known whether SePS supplementation would channel the Se into selenoamino acids, hence into selenoprotein and selenoenzyme. Since SePSs are not digestible by humans as they are non-starch polysaccharides, using the Se in these polymers in the body involves the breakdown of the polymers and their transformation by bacteria during colonic bacterial fermentation akin to bacterial fermentation of dietary fiber into absorbable short chain fatty acids (SCFAs) (Wu et al., 2023; Zainudin et al., 2023).

2.6.2 | Antioxidant effect of selenopolysaccharide

SePS itself has been shown to process antioxidant activity as measured by the ferric reducing antioxidant power (FRAP) assay and radical scavenging assays using 2,2′-azino-bis-(3-ethylbenzothiazoline-6-sulfonic acid) (ABTS), 2,2-diphenyl-1-picryhydrazyl (DPPH), and superoxide anion ($O^{2-}\cdot$) as the radical species (Gao et al., 2020; Gu et al., 2020; He et al., 2022; Q. Li et al., 2017; Lian et al., 2018; Liu et al., 2022; Xiang et al., 2022; Zhang et al., 2021). The antioxidant property could arise from seleno-groups like -SeH in the sugar structure similar to the thiol group -SH as the electron donating group in the scavenging of free radicals. Antioxidant activity determined with hydroxyl radical (HO·) was also carried out, but this is more likely due to the "sacrificial antioxidant" property of the polysaccharide or SePS due to the very high reactivity and non-specificity of HO· reaction with organic compounds, especially toward high MW ones. Some studies access the antioxidant activity of SePS at the cellular level in providing a more relevant assessment of antioxidant activity, by determining its protective effect against DNA damage in cultured cells induced by membrane-permeable oxidative chemical agents such as H_2O_2. Studies to date have indicated that the antioxidant activity of SePS is affected by many parameters, including its Se content, MW, monosaccharide composition, and polymer structure.

The three natural SePS from tea leaves (SeTPS1, SeTPS2, and SeTPS2) have stronger superoxide anion and DPPH radical scavenging activities compared to the non-selenized polysaccharides from the same tea (Wang et al., 2015). Likewise, the natural SePS from Se-enriched *Grifola frondose* (Se-GFP-22) showed significantly higher dose-dependent radical scavenging activities compared to its non-selenized polysaccharide (GFP-22) counterpart (Q. Li et al. (2017). The natural SePS from *P. ostreatus* (Se-POP-21) also showed a dose-dependent DPPH radical scavenging activity (Zhang et al., 2021). The selenol group (-SeH) in these SePS structures is analogous to the thiol group (-SH) with similar chemical properties, including exhibiting antioxidant and redox properties due to their ability to donate electrons or hydrogen atoms.

Synthetic SePS also possess stronger antioxidant activity than the parent polysaccharide. Polysaccharides from alfalfa (RAPS-2) that were chemically selenized with selenite group (Se-RAPS-2) possess superior DPPH and ABTS free radical scavenging activity compared to the parent polysaccharide (RAPS-2), and the scavenging activity of Se-RAPS-2 on ABTS radicals was twice as strong as that of RAPS-2 (Gao et al., 2020). Similarly, a synthetic SePS prepared from sweet potato tuber polysaccharide (Se-SWP) also showed greater antioxidant activity in terms of reducing capacity and free radicals scavenging activity than the parent polysaccharide (Yuan et al., 2017). These selenite groups can act as electron donors as the Se is in the lower oxidation state (Se^{4+}) thus capable of participating in redox reactions, contrasting to the non-electron donating higher Se oxidation state (Se^{6+}) found in selenate.

Of the two tea SePSs, while both SeTPS-1 and SeTPS-2 exhibited reducing power, antioxidant activity, and protective effect against H_2O_2-induced DNA damage in a cell culture, the higher Se content SeTPS-1 (23.50 μg/g) is more potent than the lower Se content SeTPS-2 (13.47 μg/g) (Gu et al., 2020). Natural SePS from *R. laevigata* Se-RLFPII with a higher Se content (21.61 μg/g) also exhibit higher

antioxidant activity than that of Se-RLFPI with a lower Se content (16.49 μg/g) (X. Liu et al., 2022). However, the two natural SePSs from pennycress (*T. arvense* L.) showed the opposite correlation. The lower Se content Se-PPS1 (13.56 μg/g) possessed stronger antioxidant activity than the higher Se content Se-PPS3 (15.36 μg/g) (Xiang et al., 2022). These and other studies (Hou et al., 2012) also reported on SePS MW and sugar compositions influencing antioxidant activity. Perhaps, it is premature to reach conclusions regarding MW differences in the antioxidant activity as some of the MW differences were small and due to the possibility of sugar composition affecting the solubility of the SePS in the antioxidant activity assays. Commonly, the antioxidant activity of SePS is found to increase along with the increase in Se content but this relation still needs to be confirmed with further research. There are also claims of synergistic effects between Se and the polysaccharide in SePS, which makes SePS more biologically active than the parent PS. While the combination of Se and polysaccharide leads to changes in the structure of polysaccharide molecules, the presence of the Se group also improves the ability of SePS to scavenge free radicals. Whether this effect is synergistic, in the sense that the antioxidant activity of the SePS is higher than that of the sums of the antioxidant activity from the Se group and PS, remains to be demonstrated.

In addition to In vitro antioxidant assays, several studies assess the antioxidant activity of SePSs in cells as well as in In vivo studies. These studies provided more direct evidence of the efficacy of the antioxidant effect of SePSs in eliminating oxidative damage in cells or biological systems. Liu et al. (2022) incubated the synthetic SePSs, Se-RLFPs, with human neuroblastoma (SH-SY5Y) to look at their protective effect on the cells from H_2O_2-induced oxidative damage. The levels of malondialdehyde (MDA) content, SOD activity, and FRAP were assessed to evaluate lipid oxidation level, antioxidant enzyme activity, and total antioxidant activity, respectively. These assessments were conducted to examin the effects of H_2O_2 its decomposition product, HO·, can initiate lipid oxidation. It clearly showed that the cells were protected by Se-RLFP2 supplementation in the culture media containing H_2O_2, with a reduction in the MDA content and markedly increased SOD activity and FRAP, all in a dose-dependent relationship (Liu et al., 2022). These results point to Se-RLFP2 potential in protecting cells from H_2O_2-induced damage, possibly by eliminating H_2O_2 prior to its decomposition.

SePS from *P. geesteranus* (SPMP-2a) was found to protect human keratinocytes (HaCaT) against H_2O_2-induced oxidative damage (Sun et al., 2017). The addition of SPMP-2a increases SOD and CAT activities and suppresses ROS accumulation in these cells in culture. SPMP-2a treatment also greatly increased the expression of B-cell lymphoma 2 (Bcl-2) protein, which is a regulator protein that regulates cell death (apoptosis), functioning in promoting cellular survival and suppressing the actions of pro-apoptotic proteins. Additionally, the addition of SPMP-2a could improve cell viability, decrease cell apoptotic rates, and reduce nuclear condensation in the HaCaT cell culture. The addition of SePS from *P. ostreatus* (Se-POP-1) in the H_2O_2-induced PC12 cell model showed that it protected H_2O_2-challenged PC12 cells against oxidative damage by improving cell membrane integrity, suppressing DNA damage, limiting the ratio of Bax/Bcl-2, and decreasing pro-apoptotic cytochrome and cleaved caspase 3, thereby arresting apoptosis (Ma et al., 2022). It was suggested that Se-POP-1 enhances the activities of GSH-Px and increases the content of GSH in the cells to protect against oxidative damage.

SePS from *O. radicata* (SPS) protected against endotoxin-induced kidney and lung damage in lipopolysaccharide (LPS)-treated mice (Gao et al., 2018). Enzymatic hydrolysate of SPS (ESPS) exhibited better antioxidant and protective effects over that of intact SPS against LPS-induced toxicities, by improving activities of GSH-Px, SOD, CAT, and total antioxidant capacity (T-AOC), facilitating inflammatory response, and reducing MDA and lactoperoxidase (LPO) contents in the kidneys and lungs in these mice. SePS from *P. igniarius* (PSeP) decreased ROS levels, MDA content as well as myeloperoxidase (MPO) activity apparently by increasing the activities of GSH-Px and CAT (Luo et al., 2021). Additionally, it also showed excellent wound healing effects In vivo in a mice model due to the ability of PSeP to suppress ROS levels in the skin. A SePS isolated from *L. edodes* (Se-L) had no effect on the production of ROS by granulocytes In vitro but, in normal (HUVEC) or malignant (HeLa) cells tests, could enhance cell viability and protect cells from oxidative stress condition (Kaleta et al., 2019).

Synthetic SePS containing Se as a reducing selenite group can also improve the antioxidant activities of the parent polysaccharide. Thus, while both *G. uralensis* polysaccharide (GUP) and its selenylated form (Se-GUP) could scavenge hydroxyl and DPPH radicals, Se-GUP shows stronger scavenging activity (Lian et al., 2018), and in In vivo antioxidant evaluation conducted with healthy Kunming mice, intra-gastric administration of GUP or Se-GUP for 14 days increases GSH-Px and SOD activities in a dose-dependent manner, with Se-GUP showing a stronger effect at a higher dose (300 mg/kg) of treatment. Both polysaccharides also suppress MDA levels both in blood serum and liver compared with the control mice with no feed intervention.

The antioxidant activity of SePS varies depending on many factors including the Se content, Se forms, monosaccharide composition, and polysaccharide

molecular weight. Besides, biological activities such as anti-inflammation, anti-diabetic, anti-tumor effects of polysaccharides are associated with or derived from the antioxidant activity. Thus, the identification of the SePS structure, evaluation of the biological activity of SePS, and establishing structure–activity relationships are paramount in advancing our knowledge in this area.

2.6.3 | Anti-tumor effects of selenopolysaccharide

The anti-tumor effect of SePS has been reported, and it might achieve this by: (i) inducing apoptosis by suppressing the expression of regulatory proteins related to apoptosis such as the Bcl-2 and caspase-3 family of proteins, (ii) inhibiting metastasis of tumor cells, (iii) inhibiting signaling pathways related to tumor development such as the mitogen-activated protein kinases signaling pathway, (iv) inhibiting cell mutation in reducing the risk of tumor formation, and (v) blocking late DNA synthesis stagnation at the S phase resulting in a decreased number of tumor cells in G1 and G0+M phases.

SeZYTP from green tea could significantly suppress the proliferation of human osteosarcoma U-2 OS cells in both MTT and lactate dehydrogenase (LDH) assays and was dose-dependent (25–200 μg/mL) (Y. Wang et al., 2013). When tested in a U-2 OS cancer xenograft model in BALB/c athymic mice, obvious tumor regression was observed as compared to model control after 28 days of oral administration of Se-ZYTP at 100, 200, and 400 μg/kg body weight per day. Additionally, during the test, the body weight in the Se-ZYTP treatment groups and control did not differ greatly, and no mice died, indicating the safety of Se-ZYTP administration. Similarly, SeTPS from another green tea significantly inhibited the proliferation of sarcoma S-180 tumor cells in a dose-dependent manner as indicated in the MTT and LDH assays. In the S180 cancer xenograft model in Kunming mice, the oral administration of SeTPS for 13 days (50–200 mg/kg body weight per day) resulted in significant tumor regression (Cheng et al., 2018). Compared to the group treated with the native non-selenium polysaccharide from the tea (TPS) at the same dose, SeTPS presented significantly higher anti-tumor activity. Additionally, the spleen and thymus indices of tumor-bearing mice were greatly increased in the SeTPS treatment, suggesting the immunomodulatory activity of SeTPS.

Se-POP3 and Se-POP 21 from *P. ostreatus* were also found to have anti-tumor effects (Zhang et al., 2021). In In vitro experiments with five human tumor cell lines (HepG2, MCF-7, SKOV3, HeLa, and PC-3), Se-POP-3 could induce apoptosis and inhibit the migration of these tumor cells (Zhang et al., 2020, 2022). This could be by disrupting the Bax/Bcl-2 protein ratio and inhibiting the epithelial-to-mesenchymal transition in tumor cells. The growth of three normal human cell lines (L02, MCF-10A, IOSE) in the same study was not affected. Treatment of A549, SKOV3, HepG2, and MCF-7 cells with Se-POP-21 could also induce apoptosis, inhibit metastasis of the A549 cells, and suppress epithelial-to-mesenchymal transition of A549 cells, but no significant effect on normal cells.

Interestingly, synthetic SePS that has a different Se form (as selenite) that is distinct from natural and enriched SePSs also processes anti-tumor activity. Synthetic Se-RAPS-2 produced by selenylation of alfalfa root polysaccharide displayed an effective antiproliferative effect on HepG-2 cells in a dose-dependent manner (Gao et al., 2020). Se-RAPS-2 has a significantly lower IC_{50} value than that of the native and parent polysaccharides (RAPS-1 and RAPS-2, respectively) on the growth of HepG-2 cells. Synthetic Se-ASP produced by the selenylation of *A. sphaerocephala* polysaccharide exhibited significantly enhanced anti-proliferation activity than that of the parent polysaccharides (ASP); the latter showed no obvious antiproliferation effect on HepG2 cells (S. Zhu et al., 2020). Synthetic sCPA produced by the selenylation of Chinese chestnut (*C. mollissima*) polysaccharide (CPA) showed a stronger antiproliferative effect on tumor cells than the parent CPA In vitro (H. Li et al., 2017). Both CPA and sCPA could induce apoptosis in HeLa and MCF-7 cells by reducing mitochondrial membrane potential, but only the sCPA could arrest cell stage in the S phase, activate caspase-3 activity, and promote ROS generation in promoting apoptosis in HeLa cells. While the mechanism is not known yet, these findings do suggest that chemically synthesized SePS could have potential use as anti-tumor drugs.

2.6.4 | Anti-diabetic effect of selenopolysaccharide

Diabetes is a chronic disease characterized by persistent hyperglycemia and accompanied by endocrine and metabolic disorders (Heindel et al., 2017). Studies suggested that the hypoglycemic activity demonstrated by some polysaccharides was intimately associated with their antioxidant activity, and both are relevant to the diabetic condition in correcting hyperglycemia and oxidative stress. The hypoglycemic activity of SePS is related to the inhibition of simple sugar (sucrose and lactose) and starch digestion. The digestion of starch is achieved by the combined action of pancreatic α-amylase, which depolymerizes the amylose and amylopectin in starch into maltose and maltose-oligosaccharides, and small intestinal mucosa α-glucosidases, which further digest these

fragments into absorbable glucose (Xiao et al., 2019). The digestion of sucrose and lactose would only involve the mucosa α-glucosidases.

ASe-TPS1 from tea and synthetic CSe-TPS1 produced by the selenylation of tea polysaccharide (TPS1) showed dose-dependent inhibition against α-glucosidase, and the inhibitory activity of both was much higher than the native polysaccharide TPS1 (J. Zhu et al., 2020). Both SeLEP-1a from *Lachnum* YM38 and its native polysaccharide LEP-a inhibited α-glucosidase activity in a dose-dependent manner (He et al., 2022). At different concentration points (0.25, 0.75, 1, 3, and 5 mg/mL reaction), the inhibitory activities of SeLEP-1a were higher than those of LEP-1a. Additionally, SeLEP-1a also inhibited α-amylase activity with an IC_{50} value of 1.22 mg/mL, which is stronger than LEP-1a with an IC_{50} value of 4.58 mg/mL. However, because of the rather high polysaccharide concentration used in the study that can affect solution viscosity imparting on enzyme activity, the conclusion is premature.

More direct evidence of the anti-diabetic properties can be obtained with animal studies. Selenopolysaccharides from *F. fomentarius* significantly reduce blood glucose levels, decrease HbA1c levels, and improve insulin secretion and body weight in a rat study after 28 days of oral administration of these polysaccharides to diabetic rats (Keshavarz-Rezaei et al., 2022). A lipid microemulsion formulated to contain SePS was significantly more effective. This study points to the anti-diabetic effect of SePS even though the mechanism is not known, which might involve inhibition of α-amylase/α-glucosidases and/or increases in the animal body Se status or both.

Synthetic SemCVP-1S produced by the selenylation of *C. ventricosum* polysaccharide mCVP-IS exhibited anti-hyperglycemic activity by lowering blood glucose levels in streptozotocin-induced diabetic mice (Y. Liu et al., 2017). In a 30-day long experiment, 6 normal mice were used as control and 48 streptozotocin-induced diabetic mice were randomly distributed into nine groups and treated with glibenclamide or different polysaccharides (mCVP-1S, SemCVP-1S with low/medium/high Se contents) at 0.2 g/kg per day or 2.0 g/kg per day. Body weight, glucose levels, serum concentrations of total cholesterol, triglycerides, low-density lipoprotein cholesterol, high-density lipoprotein cholesterol, and levels of GSH-PX, SOD, CAT, and MDA were determined to evaluate the effect of SemCVP-1s administration. Interestingly, SemCVP-1S with medium Se content (1.54 mg/g) exhibited superior anti-hyperglycemic activity than that of SemCVP-1S with low (1.18 mg/g) and high (1.86 mg/g) Se contents based on the levels of these factors. The authors speculated that differences in the tertiary structure of the SemCVPs due to differences in the H_2SeO_3 content on these polysaccharides might cause these differences, as it has been demonstrated that the triple-helix structure of polysaccharides is related to certain biological activities (F. Liu et al., 2017).

2.6.5 | Intestinal barrier enhancement and gut microbiota regulation

Inflammatory bowel disease is a spectrum of chronic, nonspecific inflammatory diseases of the gastrointestinal tract and includes ulcerative colitis and Crohn's disease. In an interesting study by Zhao et al. (2022), SeTP from tea was shown to enhance the integrity of the intestinal mucosal barrier in dextran sodium sulfate (DSS)-induced colitis mice, by up-regulating the tight junction protein expression. Besides, it was also found that SeTP could modulate the gut microbiota by up-regulating the proliferation of beneficial bacteria, including *Bifidobacterium*, *Lactobacillus, and norank_f_Muribaculaceae*, and down-regulating pathogenic microorganisms, including *Akkermansia*, *Desulfovibrio*, *Parasutterella*, and *Romboutsia* in the DSS-induced colitis mice. The decrease in colon length, weight loss, and increase in disease activity index score, which includes assessment of weight, stool consistency, and occurrence of intestinal bleeding, can be induced by DSS in these mice. Oral administration of SeTP alleviates these negative changes in the mice. Furthermore, SeTP also attenuated the damage to the mice's colonic mucosal barrier via up-regulating the expression levels of claudin-1, occludin, and zona occludens-1. Oral intake of SeTP administered to the mice by gavage increased the Se content, reduced oxidative stress by suppressing MDA levels, enhanced the antioxidant capacity by promoting the activities of SOD and GSH-Px, and down-regulated the contents of proinflammatory cytokines (interferon-γ, interleukin-1β, Interleukin-6, tumor necrosis factor-α, and lipopolysaccharides) and MPO activity in the colonic tissue.

3 | EXISTENCE OF SELENOFLAVONOIDS

Flavonoids are known to play an important role in health promotion and disease prevention due to their antioxidative and biological activities expressing as anti-inflammatory, anti-diabetic, anti-carcinogenic, and anti-mutagenic (Panche et al., 2016). The exploration of the interaction between Se and flavonoid production in plants as well as the probable existence of SeFs would open new research and application prospects.

With the advent of the discovery of selenosugars and SePSs, interest has also been focused on the existence

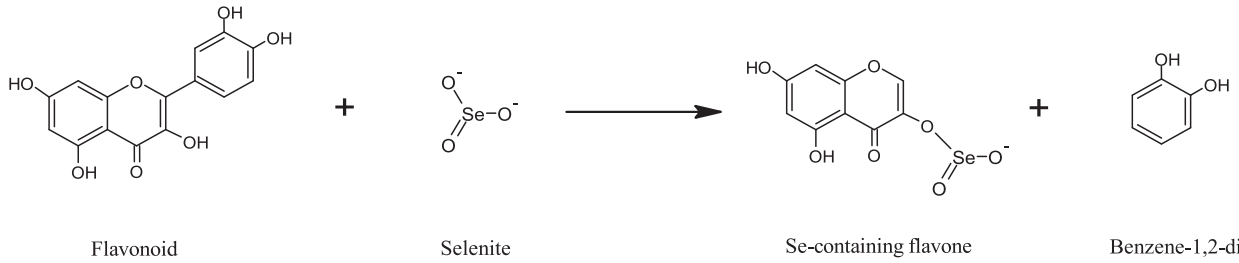

FIGURE 6 Proposed biosynthetic route for the biosynthesis of Se-containing flavone in *Camellia sinensis*. $HSeO_3^-$ can be added to the -OH group on the C-2 of the 2-phenylchromone in the flavone (Fan et al., 2022).

of SeFs. While there are several reports of Se enrichment in partially purified flavonoid fractions from foods, notably from tea, this has not been directly confirmed from structural identification of the SeFs.

Fan et al. (2022) successfully isolated a Se-containing 5,7-dihydroxychromone (Se-DHC) from Se-enriched green tea using high-speed counter-current chromatography (HSCCC). Characterization by FT-IR, ^{1}H-NMR, and UHPLC-Q-Orbitrap revealed a selenite group (SeO_3^-) on the C3 position of the 5,7-dihydroxychromone structure (Figure 6). In the FT-IR analysis, there were two novel characteristic absorption peaks at 602 and 685 cm^{-1}, attributed to the presence of Se-O-C and Se = O bonds in the flavone, indicating the hydroxyl group on C-3 was substituted with inorganic Se and transformed to organic Se compound. Based on the results of ^{1}H-NMR, it was speculated that the high density of electron cloud of oxygen at 3-OH in the benzopyran ring enables the hydroxyl group with strong nucleophilicity, which promotes the attack to $HSeO_3^-$ and esterification.

Evaluation of Se-DHC anti-inflammatory activity with RAW 264.7 cells showed Se-DHC is devoid of cytotoxic effects and exhibited superior immunomodulatory properties compared to flavone when the concentration remained below 60 μmol/L. Se-DHC could also protect RAW 264.7 macrophages against inflammation induced by LPS by downregulating the expression of LPS-triggered inflammatory mediators, notably tumor necrosis factor-α, interleukin-6, and nitrous oxide, with the optimal dosage being 40 μmol/L. Furthermore, Se-DHC appeared to play a pivotal role in mitigating severe inflammatory injury by activating the classical IL-6 signaling pathway, thereby inducing sustained STAT3 activation and subsequently enhancing the release of IL-10. This, in turn, contributed to the restoration of cellular morphology and the repair of damaged nuclei in LPS-stimulated RAW 264.7 cells.

In addition to the discovery of Se-containing flavone, an Se-enriched polyphenol fraction (Se-TPP) with a Se content at 0.392 μg/g was isolated from Se-rich green tea of *Camellia sinensis* L. (Ziyang tea) (Ren et al., 2014)). The polyphenols in this fraction were identified as epigallocatechin gallate (28.2%), epigallocatechin (5.7%), and epicatechin gallate (5.6%). At the same time, a SePS mainly composed of neutral glucose (31.4%), arabinose (23.5%), and galactose (21.87%) was also isolated from the same tea, and it was found that the SePS had a Se content of 1.517 μg/g, which was much higher than that of the Se-TPP. The results of the antioxidant evaluation of both Se-containing compounds showed that SeTPP and SePS exhibited a reducing effect against ferric ions and strong radical scavenging antioxidant activity against DPPH radicals, hydroxyl radicals, and superoxide anions. Due to the polyphenol contents, Se-TPP showed a markedly higher reducing capacity and stronger scavenging activity than the SePS.

SeFs can also be obtained by chemical synthesis methods. Selenized chrysin (SeChry) and 3,7,3′,4′-tetramethylquercetin (SePQue) derivatives (Figure 7) were synthesized by Martins et al. (2015) to study the properties of SeF. Quercetin was initially methylated with dimethylsulfate to protect the 3, 7, 3′, and 4′ hydroxyl groups, followed by a microwave-based synthetic method using Woollins' reagent (an organic compound containing phosphorus and Se) as the Se source that allows an efficient conversion of C-4 carbonyl groups to selenocarbonyl. Chrysin can be directly selenized by reaction with the Woollins' reagent without protection to give SeChry with a C-4 selenocarbonyl. The selenocarbonyl entity was confirmed by mass spectrometry of the products and ^{77}Se-NMR, in which signals at 768.3 and 815.2 ppm were observed for SePQue and SeChry. Evaluation of the biological activity of SeChry and SePQue showed that in addition to the improved DPPH radical scavenging and potential GPx-like activities, both SeChry and SePQue were more cytotoxic by comparison to their oxygen and sulfur congeners. SeChry showed an enhanced cytotoxic activity with mean IC_{50} values 3-fold and 18-fold lower than those observed for cisplatin (a platinum antineoplastic agent) and chrysin. Both Se-derivatives showed an ability to overcome the resistance to cisplatin and multiple drugs. Notably, SeChry and SePQue could efficiently inhibit the clonal expansion and suppress TrxR activity

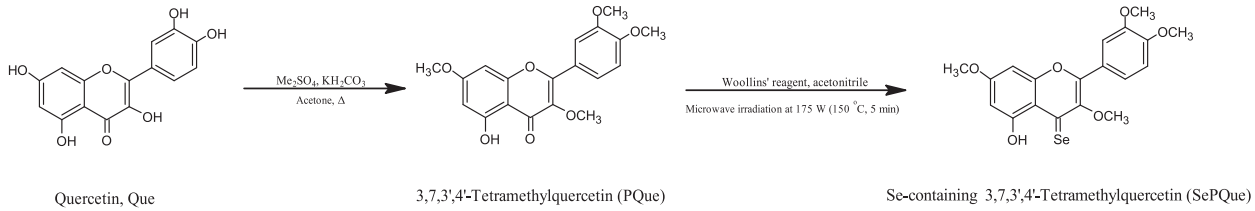

(a) Synthetic route for the chalcogenation of protected quercetin

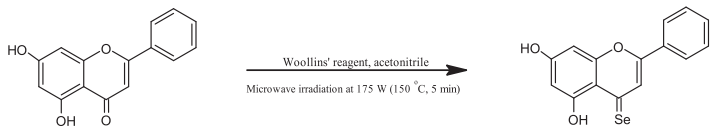

(b) Synthetic route for chrysin direct chalcogenation

FIGURE 7 Chemical synthesis of Se-containing (A) 3,7,3′,4′-tetramethylquercetin (SePQue) and (B) chrysin (SeChry) (Martins et al., 2015).

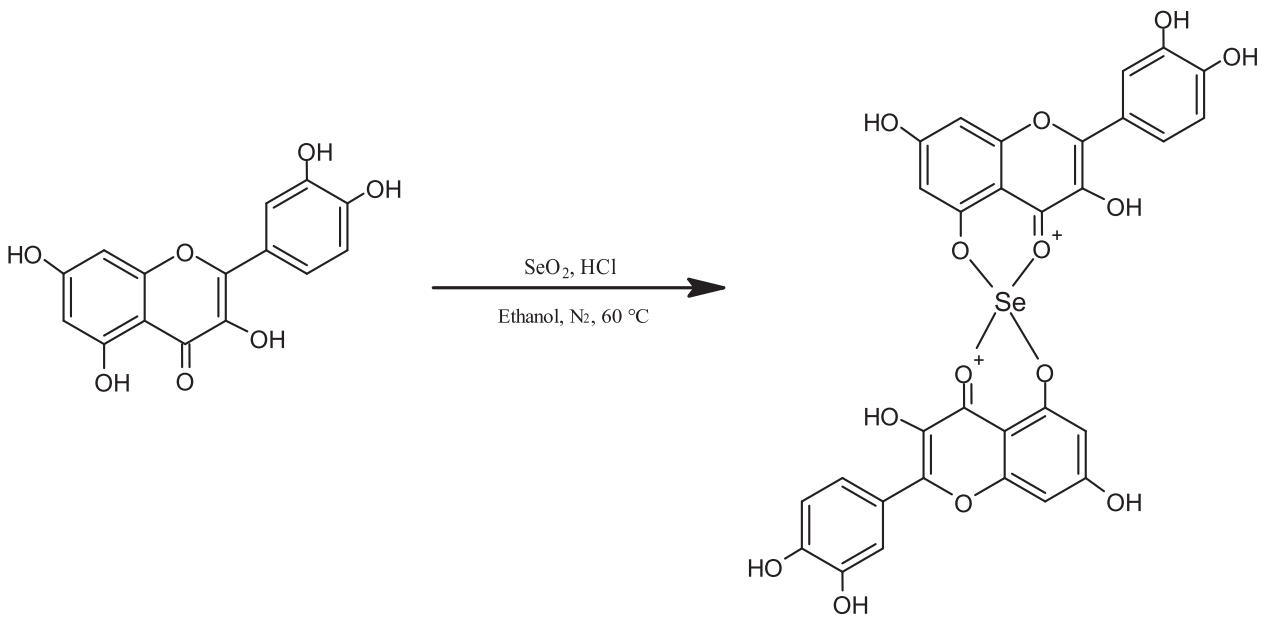

FIGURE 8 Chemical synthesis of Se-quercetin complex. (Zhang & Chen, 2012).

in MCF-7 human mammary cancer cells and further lead to apoptotic cell death. Interestingly, these Se-derivatives possess higher selectivity indexes in comparison to their oxo and thio-analogues. Besides these, a Se-quercetin complex (SEQC) was synthesized by Zhang and Chen (2012) via the reaction between quercetin and selenium dioxide (SeO_2) in ethanol catalyzed by concentrated hydrogen chloride under a condition of 60°C for 12 h with the protection of nitrogen (Figure 8). The structure of SEQC was identified by IR, ^{1}H-NMR, and LC-MS. The bond of Se-O was identified at 780 cm^{-1} in IR spectroscopy, and it was speculated that the mole ratio of Se to quercetin was 1:2, and the proposed structure of this complex is shown in Figure 8. All these studies suggested

that selenized flavonoids could be potential candidates for the development of new anti-cancer agents for cancer chemotherapy.

Thus, there is a need to explore the existence and biosynthesis mechanisms of SeF, to evaluate its potential biological activity to discover its nutritional and medical values.

4 | CONCLUSION AND PERSPECTIVES

The discovery of selenosugars and SePSs in plants and fungi is a significant advancement in organic Se research because it opens a vast new source of organic Se from foods. In addition, as a new organic Se source apart from the selenoamino acids and selenoproteins, their biological effect in promoting human health is only just beginning to be documented and understood. This is an area of research that might lead to the development of new functional products in promoting human health and disease prevention. While identification of SeFs was preliminary, the fact that Se-5,7-dihydroxychromone was isolated from tea points strongly to their possible existence. Selenoflavonoids would represent a very interesting new class of organic Se compounds with high therapeutic potential due to the strong antioxidant activity inherent in flavonoids, besides as another new source of organic Se. Therefore, future research in this area should continue with the identification of SePSs and SeFs in various plants, fungi, and other foods and structural characterization of the organic Se forms, determination of their bioavailability and how they are processed in the body, and investigation of the relationship between the organic Se forms and their biological properties in the body and in the colon arising from bacterial fermentation.

AUTHOR CONTRIBUTIONS

Ziqi Qi: Conceptualization; data curation; formal analysis; investigation; methodology; visualization; writing—original draft; writing—review and editing. **Alex Duan**: Supervision; formal analysis; investigation; writing—review and editing. **Ken Ng**: Supervision; conceptualization; formal analysis; writing—review and editing; investigation; methodology; project administration.

ACKNOWLEDGMENTS

None.

CONFLICT OF INTEREST STATEMENT

The authors declare no conflicts of interest.

DATA AVAILABILITY STATEMENT

Data will be made available on request.

ORCID

Ken Ng https://orcid.org/0000-0002-1843-0506

REFERENCES

Alves, C. S., Vicentini, R., Duarte, G. T., Pinoti, V. F., Vincentz, M., & Nogueira, F. T. (2017). Genome-wide identification and characterization of tRNA-derived RNA fragments in land plants. *Plant Molecular Biology*, *93*(1-2), 35–48. https://doi.org/10.1007/s11103-016-0545-9

Araujo, J. M., Fortes-Silva, R., Pola, C. C., Yamamoto, F. Y., Gatlin, D. M., 3rd, & Gomes, C. L. (2021). Delivery of selenium using chitosan nanoparticles: Synthesis, characterization, and antioxidant and growth effects in Nile tilapia (Orechromis niloticus). *PLoS ONE*, *16*(5), e0251786. https://doi.org/10.1371/journal.pone.0251786

Arshad, M. A., Ebeid, H. M., & Hassan, F.-U. (2021). Revisiting the effects of different dietary sources of selenium on the health and performance of dairy animals: A review. *Biological Trace Element Research*, *199*(9), 3319–3337. https://doi.org/10.1007/s12011-020-02480-6

Aureli, F., Ouerdane, L., Bierla, K., Szpunar, J., Prakash, N. T., & Cubadda, F. (2012). Identification of selenosugars and other low-molecular weight selenium metabolites in high-selenium cereal crops. *Metallomics*, *4*(9), 968–978. https://doi.org/10.1039/c2mt20085f

Berthiller, F., Werner, U., Sulyok, M., Krska, R., Hauser, M.-T., & Schuhmacher, R. (2006). Liquid chromatography coupled to tandem mass spectrometry (LC-MS/MS) determination of phase II metabolites of the mycotoxin zearalenone in the model plant *Arabidopsis thaliana*. *Food Additives and Contaminants*, *23*(11), 1194–1200. https://doi.org/10.1080/02652030600778728

Blazevic, I., Montaut, S., Burcul, F., Olsen, C. E., Burow, M., Rollin, P., & Agerbirk, N. (2020). Glucosinolate structural diversity, identification, chemical synthesis and metabolism in plants. *Phytochemistry*, *169*, 112100. https://doi.org/10.1016/j.phytochem.2019.112100

Chang, C.-W., Lur, H.-S., Lu, M.-K., & Cheng, J.-J. (2013). Sulfated polysaccharides of *Armillariella mellea* and their anti-inflammatory activities via NF-κB suppression. *Food Research International*, *54*(1), 239–245. https://doi.org/10.1016/j.foodres.2013.07.005

Chaplin, M. F. Carbohydrate Analysis. In *Reviews in Cell Biology and Molecular Medicine*. https://doi.org/10.1002/3527600906.mcb.200300011

Chen, L., & Huang, G. (2018). The antiviral activity of polysaccharides and their derivatives. *International Journal of Biological Macromolecules*, *115*, 77–82. https://doi.org/10.1016/j.ijbiomac.2018.04.056

Chen, T., Li, B., Li, Y., Zhao, C., Shen, J., & Zhang, H. (2011). Catalytic synthesis and antitumor activities of sulfated polysaccharide from *Gynostemma pentaphyllum* Makino. *Carbohydrate Polymers*, *83*(2), 554–560. https://doi.org/10.1016/j.carbpol.2010.08.024

Cheng, J., Song, J., Wei, H., Wang, Y., Huang, X., Liu, Y., Lu, N., He, L., Lv, G., Ding, H., Yang, S., & Zhang, Z. (2020). Structural characterization and hypoglycemic activity of an intracellular

polysaccharide from *Sanghuangporus sanghuang* mycelia. *International Journal of Biological Macromolecules*, *164*, 3305–3314. https://doi.org/10.1016/j.ijbiomac.2020.08.202

Cheng, L., Chen, L., Yang, Q., Wang, Y., & Wei, X. (2018). Antitumor activity of Se-containing tea polysaccharides against sarcoma 180 and comparison with regular tea polysaccharides and Se-yeast. *International Journal of Biological Macromolecules*, *120*(Pt A), 853–858. https://doi.org/10.1016/j.ijbiomac.2018.08.154

Chen, X. W., Zheng, Y. Y., & Ouyang, J. M. (2023). Sulfated Undaria pinnatifida Polysaccharide Promotes Endocytosis of Nano-Calcium Oxalate Dihydrate by Repairing Subcellular Organelles in HK-2 Cells. *Antioxidants (Basel)*, *12*(5), 1015. https://doi.org/10.3390/antiox12051015

Cooper, C. A., Gasteiger, E., & Packer, N. H. (2001). GlycoMod–a software tool for determining glycosylation compositions from mass spectrometric data. *Proteomics*, *1*(2), 340–349. https://doi.org/10.1002/1615-9861(200102)1:2⟨340::AID-PROT340⟩3.0.CO;2-B

Dong, Z., Liu, Y., Dong, G., & Wu, H. (2021). Effect of boiling and frying on the selenium content, speciation, and in vitro bioaccessibility of selenium-biofortified potato (*Solanum tuberosum* L.). *Food Chemistry*, *348*, 129150. https://doi.org/10.1016/j.foodchem.2021.129150

Dong, Z., Xiao, Y., & Wu, H. (2021). Selenium accumulation, speciation, and its effect on nutritive value of *Flammulina velutipes* (Golden needle mushroom). *Food Chemistry*, *350*, 128667. https://doi.org/10.1016/j.foodchem.2020.128667

Duan, W. X., Yang, X. H., Zhang, H. F., Feng, J., & Zhang, M. Y. (2022). Chemical structure, hypoglycemic activity, and mechanism of action of selenium polysaccharides. *Biological Trace Element Research*, *200*(10), 4404–4418. https://doi.org/10.1007/s12011-021-03035-z

Dumont, E., Vanhaecke, F., & Cornelis, R. (2006). Selenium speciation from food source to metabolites: A critical review. *Analytical and Bioanalytical Chemistry*, *385*(7), 1304–1323. https://doi.org/10.1007/s00216-006-0529-8

El Hanafi, K., Pedrero, Z., Ouerdane, L., Marchan Moreno, C., Queipo-Abad, S., Bueno, M., Pannier, F., Corns, W. T., Cherel, Y., Bustamante, P., & Amouroux, D. (2022). First time identification of selenoneine in seabirds and its potential role in mercury detoxification. *Environmental Science & Technology*, *56*(5), 3288–3298. https://doi.org/10.1021/acs.est.1c04966

El Mehdawi, A. F., Jiang, Y., Guignardi, Z. S., Esmat, A., Pilon, M., Pilon-Smits, E. A. H., & Schiavon, M. (2018). Influence of sulfate supply on selenium uptake dynamics and expression of sulfate/selenate transporters in selenium hyperaccumulator and nonhyperaccumulator Brassicaceae. *New Phytologist*, *217*(1), 194–205. https://doi.org/10.1111/nph.14838

Fan, Z., Jia, W., Du, A., Xia, Z., Kang, J., Xue, L., Sun, Y., & Shi, L. (2022). Discovery of Se-containing flavone in Se-enriched green tea and the potential application value in the immune regulation. *Food Chemistry*, *394*, 133468. https://doi.org/10.1016/j.foodchem.2022.133468

Feng, M., Wang, X., Xiong, H., Qiu, T., & Sun, Y. (2021). Anti-inflammatory effects of three selenium-enriched brown rice protein hydrolysates in LPS-induced RAW264.7 macrophages via NF-κB/MAPKs signaling pathways. *Journal of Functional Foods*, *76*, 104320. https://doi.org/10.1016/j.jff.2020.104320

Ferro, C., Florindo, H. F., & Santos, H. A. (2021). Selenium Nanoparticles for Biomedical Applications: From Development and Characterization to Therapeutics. *Advanced Healthcare Materials*, *10*(16), e2100598. https://doi.org/10.1002/adhm.202100598

Gandin, V., Khalkar, P., Braude, J., & Fernandes, A. P. (2018). Organic selenium compounds as potential chemotherapeutic agents for improved cancer treatment. *Free Radical Biology & Medicine*, S0891584918308116. https://doi.org/10.1016/j.freeradbiomed.2018.05.001

Gao, P., Bian, J., Xu, S., Liu, C., Sun, Y., Zhang, G., Li, D., & Liu, X. (2020). Structural features, selenization modification, antioxidant and anti-tumor effects of polysaccharides from alfalfa roots. *International Journal of Biological Macromolecules*, *149*, 207–214. https://doi.org/10.1016/j.ijbiomac.2020.01.239

Gao, W., Zhang, N., Li, S., Li, S., Zhu, S., Cong, X., Cheng, S., Barba, F. J., & Zhu, Z. (2022). Polysaccharides in selenium-enriched tea: Extraction performance under innovative technologies and antioxidant activities. *Foods*, *11*(17), 2545. https://doi.org/10.3390/foods11172545

Gao, Z., Chen, J., Qiu, S., Li, Y., Wang, D., Liu, C., Li, X., Hou, R., Yue, C., Liu, J., Li, H., & Hu, Y. (2016). Optimization of selenylation modification for garlic polysaccharide based on immune-enhancing activity. *Carbohydrate Polymers*, *136*, 560–569. https://doi.org/10.1016/j.carbpol.2015.09.065

Gao, Z., Zhang, C., Liu, H., Zhu, Y., Ren, Z., Jing, H., Li, S., Zhang, J., Liu, X., & Jia, L. (2018). The characteristics and antioxidation of *Oudemansiella radicata* selenium polysaccharides on lipopolysaccharide-induced endo-toxemic mice. *International Journal of Biological Macromolecules*, *116*, 753–764. https://doi.org/10.1016/j.ijbiomac.2018.05.078

Gencheva, R., Cheng, Q., & Arner, E. S. (2022). Thioredoxin reductase selenoproteins from different organisms as potential drug targets for treatment of human diseases. *Free Radical Biology and Medicine*, *190*, 320–338. https://doi.org/10.1016/j.freeradbiomed.2022.07.020

Geng, Y., Xing, L., Sun, M., & Su, F. (2016). Immunomodulatory effects of sulfated polysaccharides of pine pollen on mouse macrophages. *Int J Biol Macromol*, *91*, 846–855. https://doi.org/10.1016/j.ijbiomac.2016.06.021

Górska, S., Maksymiuk, A., & Turło, J. (2021). Selenium-containing polysaccharides—Structural diversity, biosynthesis, chemical modifications and biological activity. *Applied Sciences*, *11*(8), 3717. https://doi.org/10.3390/app11083717

Gu, Y., Qiu, Y., Wei, X., Li, Z., Hu, Z., Gu, Y., Zhao, Y., Wang, Y., Yue, T., & Yuan, Y. (2020). Characterization of selenium-containing polysaccharides isolated from selenium-enriched tea and its bioactivities. *Food Chemistry*, *316*, 126371. https://doi.org/10.1016/j.foodchem.2020.126371

Guo, P., Wang, Q., Liu, J., Liu, L., Zhao, P., Cao, Y., Liu, Y., Qi, C., & Liu, Y. (2013). Preparation of two organoselenium compounds and their induction of apoptosis to SMMC-7221 cells. *Biological Trace Element Research*, *154*, 304–311. https://doi.org/10.1007/s12011-013-9715-7

He, N., Shi, X., Zhao, Y., Tian, L., Wang, D., & Yang, X. (2013). Inhibitory effects and molecular mechanisms of selenium-containing tea polysaccharides on human breast cancer MCF-7 cells. *Journal of Agricultural and Food Chemistry*, *61*(3), 579–588. https://doi.org/10.1021/jf3036929

He, Y., Chen, H., Ye, Z., Zhang, X., Ye, H., & Ye, M. (2022). Structural characterization and bioactivities of a novel polysaccharide obtained from Lachnum YM38 together with its zinc and selenium

derivatives. *Process Biochemistry*, *122*, 282–298. https://doi.org/10.1016/j.procbio.2022.08.035

Heindel, J. J., Blumberg, B., Cave, M., Machtinger, R., Mantovani, A., Mendez, M. A., Nadal, A., Palanza, P., Panzica, G., Sargis, R., Vandenberg, L. N., & Vom Saal, F. (2017). Metabolism disrupting chemicals and metabolic disorders. *Reproductive Toxicology*, *68*, 3–33. https://doi.org/10.1016/j.reprotox.2016.10.001

Hildebrand, J., Greiner, A., Drexler, H., & Goen, T. (2020). Determination of eleven small selenium species in human urine by chromatographic-coupled ICP-MS methods. *Journal of Trace Elements in Medicine and Biology*, *61*, 126519. https://doi.org/10.1016/j.jtemb.2020.126519

Hou, Y., Wang, J., Jin, W., Zhang, H., & Zhang, Q. (2012). Degradation of Laminaria japonica fucoidan by hydrogen peroxide and antioxidant activities of the degradation products of different molecular weights. *Carbohydr Polym*, *87*(1), 153–159. https://doi.org/10.1016/j.carbpol.2011.07.031

Hu, B., Liang, D., Liu, J., Lei, L., & Yu, D. (2014). Transformation of heavy metal fractions on soil urease and nitrate reductase activities in copper and selenium co-contaminated soil. *Ecotoxicology and Environmental Safety*, *110*, 41–48. https://doi.org/10.1016/j.ecoenv.2014.08.007

Huang, S., Yang, W., & Huang, G. (2020). Preparation and activities of selenium polysaccharide from plant such as *Grifola frondosa*. *Carbohydrate Polymers*, *242*, 116409. https://doi.org/10.1016/j.carbpol.2020.116409

Jiang, W., He, S., Su, D., Ye, M., Zeng, Q., & Yuan, Y. (2022). Synthesis, characterization of tuna polypeptide selenium nanoparticle, and its immunomodulatory and antioxidant effects in vivo. *Food Chemistry*, *383*, 132405. https://doi.org/10.1016/j.foodchem.2022.132405

Jiang, Z., Chi, J., Li, H., Wang, Y., Liu, W., & Han, B. (2021). Effect of chitosan oligosaccharide-conjugated selenium on improving immune function and blocking gastric cancer growth. *European Journal of Pharmacology*, *891*, 173673. https://doi.org/10.1016/j.ejphar.2020.173673

Kaleta, B., Gorski, A., Zagozdzon, R., Cieslak, M., Kazmierczak-Baranska, J., Nawrot, B., Klimaszewska, M., Malinowska, E., Gorska, S., & Turlo, J. (2019). Selenium-containing polysaccharides from Lentinula edodes-Biological activity. *Carbohydrate Polymers*, *223*, 115078. https://doi.org/10.1016/j.carbpol.2019.115078

Keshavarz-Rezaei, M., Hatamian-Zarmi, A., Alvandi, H., Ebrahimi-Hosseinzadeh, B., & Mokhtari-Hosseini, Z. B. (2022). The HbA1c and blood glucose response to selenium-rich polysaccharide from *Fomes fomentarius* loaded solid lipid nanoparticles as a potential antidiabetic agent in rats. *Biomaterials Advances*, *140*, 213084. https://doi.org/10.1016/j.bioadv.2022.213084

Khanam, A., & Platel, K. (2016). Bioaccessibility of selenium, selenomethionine and selenocysteine from foods and influence of heat processing on the same. *Food Chemistry*, *194*, 1293–1299. https://doi.org/10.1016/j.foodchem.2015.09.005

Kobayashi, Y., Ogra, Y., Ishiwata, K., Takayama, H., Aimi, N., & Suzuki, K. T. (2002). Selenosugars are key and urinary metabolites for selenium excretion within the required to low-toxic range. *Proceedings of the National Academy of Sciences*, *99*(25), 15932–15936. https://doi.org/10.1073/pnas.252610699

Lajin, B., Kuehnelt, D., Jensen, K. B., & Francesconi, K. A. (2016). Investigating the intra-individual variability in the human metabolic profile of urinary selenium. *Journal of Trace Elements in Medicine and Biology*, *37*, 31–36. https://doi.org/10.1016/j.jtemb.2016.06.008

Lei, X. G., Combs, G. F., jr., Sunde, R. A., Caton, J. S., Arthington, J. D., & Vatamaniuk, M. Z. (2022). Dietary selenium across species. *Annual Review of Nutrition*, *42*, 337–375. https://doi.org/10.1146/annurev-nutr-062320-121834

Li, H., Wang, Y., Wang, C., Zhang, S., Li, S., Zhou, G., Wang, S., & Zhang, J. (2017). Extraction, selenylation modification and antitumor activity of the glucan from *Castanea mollissima* Blume. *Glycoconj J*, *34*(2), 207–217. https://doi.org/10.1007/s10719-016-9753-4

Li, Q., Wang, W., Zhu, Y., Chen, Y., Zhang, W., Yu, P., Mao, G., Zhao, T., Feng, W., Yang, L., & Wu, X. (2017). Structural elucidation and antioxidant activity a novel Se-polysaccharide from Se-enriched *Grifola frondosa*. *Carbohydrate Polymers*, *161*, 42–52. https://doi.org/10.1016/j.carbpol.2016.12.041

Lian, K. X., Zhu, X. Q., Chen, J., Liu, G., & Gu, X. L. (2018). Selenylation modification: Enhancement of the antioxidant activity of a *Glycyrrhiza uralensis* polysaccharide. *Glycoconjugate Joural*, *35*(2), 243–253. https://doi.org/10.1007/s10719-018-9817-8

Liao, S. F., Brown, K. R., Stromberg, A. J., Burris, W. R., Boling, J. A., & Matthews, J. C. (2011). Dietary supplementation of selenium in inorganic and organic forms differentially and commonly alters blood and liver selenium concentrations and liver gene expression profiles of growing beef heifers. *Biological Trace Element Research*, *140*(2), 151–169. https://doi.org/10.1007/s12011-010-8685-2

Liu, F., Zhu, Z. Y., Sun, X., Gao, H., & Zhang, Y. M. (2017). The preparation of three selenium-containing *Cordyceps militaris* polysaccharides: Characterization and anti-tumor activities. *International Journal of Biological Macromolecules*, *99*, 196–204. https://doi.org/10.1016/j.ijbiomac.2017.02.064

Liu, X., Gao, Y., Li, D., Liu, C., Jin, M., Bian, J., Lv, M., Sun, Y., Zhang, L., & Gao, P. (2018). The neuroprotective and antioxidant profiles of selenium-containing polysaccharides from the fruit of *Rosa laevigata*. *Food Funct*, *9*(3), 1800–1808. https://doi.org/10.1039/c7fo01725a

Liu, X., Liu, J., Liu, C., Zhang, X., Zhao, Z., Xu, J., Zhang, X., Zhou, K., Gao, P., & Li, D. (2022). Selenium-containing polysaccharides isolated from *Rosa laevigata* Michx fruits exhibit excellent antioxidant and neuroprotective activity in vitro. *International Journal of Biological Macromolecules*, *209*(Pt A), 1222–1233. https://doi.org/10.1016/j.ijbiomac.2022.04.146

Liu, Y., Sun, J., Rao, S., Su, Y., Li, J., Li, C., Xu, S., & Yang, Y. (2013). Antidiabetic activity of mycelia selenium-polysaccharide from *Catathelasma ventricosum* in STZ-induced diabetic mice. *Food and Chemical Toxicology*, *62*, 285–291. https://doi.org/10.1016/j.fct.2013.08.082

Liu, Y., You, Y., Li, Y., Zhang, L., Yin, L., Shen, Y., Li, C., Chen, H., Chen, S., Hu, B., & Chen, D. (2017). The characterization, selenylation and antidiabetic activity of mycelial polysaccharides from *Catathelasma ventricosum*. *Carbohydrate Polymers*, *174*, 72–81. https://doi.org/10.1016/j.carbpol.2017.06.050

Luo, L., Wang, Y., Zhang, S., Guo, L., Jia, G., Lin, W., Gao, Z., Gao, Y., & Sun, T. (2021). Preparation and characterization of selenium-rich polysaccharide from *Phellinus igniarius* and its effects on wound healing. *Carbohydrate Polymers*, *264*, 117982. https://doi.org/10.1016/j.carbpol.2021.117982

Ma, L., Liu, J., Liu, A., & Wang, Y. (2022). Cytoprotective effect of selenium polysaccharide from *Pleurotus ostreatus* against H2O2-

induced oxidative stress and apoptosis in PC12 cells. *Arabian Journal of Chemistry*, *15*(4), 103686. https://doi.org/10.1016/j.arabjc.2022.103686

Malinowska, E., Klimaszewska, M., Straczek, T., Schneider, K., Kapusta, C., Podsadni, P., Lapienis, G., Dawidowski, M., Kleps, J., Gorska, S., Pisklak, D. M., & Turlo, J. (2018). Selenized polysaccharides—Biosynthesis and structural analysis. *Carbohydrate Polymers*, *198*, 407–417. https://doi.org/10.1016/j.carbpol.2018.06.057

Martins, I. L., Charneira, C., Gandin, V., Ferreira da Silva, J. L., Justino, G. C., Telo, J. P., Vieira, A. J., Marzano, C., & Antunes, A. M. (2015). Selenium-containing chrysin and quercetin derivatives: Attractive scaffolds for cancer therapy. *Journal of Medicinal Chemistry*, *58*(10), 4250–4265. https://doi.org/10.1021/acs.jmedchem.5b00230

Medicine, I. O. (2000). *Dietary Reference Intakes for Vitamin C, Vitamin E, Selenium, and Carotenoids*. The National Academies Press. https://doi.org/10.17226/9810

Mikkelsen, M. D., Harholt, J., Westereng, B., Domozych, D., Fry, S. C., Johansen, I. E., Fangel, J. U., Łężyk, M., Feng, T., & Nancke, L. (2021). Ancient origin of fucosylated xyloglucan in charophycean green algae. *Communications Biology*, *4*(1), 754. https://doi.org/10.1038/s42003-021-02277-w

Mizutani, M., Nakanishi, H., Ema, J., Ma, S. J., Noguchi, E., Inohara-Ochiai, M., Fukuchi-Mizutani, M., Nakao, M., & Sakata, K. (2002). Cloning of beta-primeverosidase from tea leaves, a key enzyme in tea aroma formation. *Plant Physiology*, *130*(4), 2164–2176. https://doi.org/10.1104/pp.102.011023

Nayak, V., Singh, K. R., Singh, A. K., & Singh, R. P. (2021). Potentialities of selenium nanoparticles in biomedical science. *New Journal of Chemistry*, *45*(6), 2849–2878. https://doi.org/10.1039/d0nj05884j

Nicholson, J. L., Toh, P., Alfulaij, N., Berry, M. J., & Torres, D. J. (2022). New insights on selenoproteins and neuronal function. *Free Radical Biology and Medicine*, *190*, 55–61. https://doi.org/10.1016/j.freeradbiomed.2022.07.021

Ouerdane, L., Aureli, F., Flis, P., Bierla, K., Preud'Homme, H., Cubadda, F., & Szpunar, J. (2013). Comprehensive speciation of low-molecular weight selenium metabolites in mustard seeds using HPLC–electrospray linear trap/orbitrap tandem mass spectrometry. *Metallomics*, *5*(9), 1294–1304. https://doi.org/10.1039/c3mt00113j

Panche, A. N., Diwan, A. D., & Chandra, S. R. (2016). Flavonoids: An overview. *Journal of Nutritional Science*, *5*, e47. https://doi.org/10.1017/jns.2016.41

Pedrero, Z., Elvira, D., Camara, C., & Madrid, Y. (2007). Selenium transformation studies during broccoli (*Brassica oleracea*) growing process by liquid chromatography-inductively coupled plasma mass spectrometry (LC-ICP-MS). *Analytica Chimica Acta*, *596*(2), 251–256. https://doi.org/10.1016/j.aca.2007.05.067

Pedrero, Z., & Madrid, Y. (2009). Novel approaches for selenium speciation in foodstuffs and biological specimens: A review. *Analytica Chimica Acta*, *634*(2), 135–152. https://doi.org/10.1016/j.aca.2008.12.026

Pérez, M. B., Maniero, M. Á., Londonio, A., Smichowski, P., & Wuilloud, R. G. (2018). Effects of common cooking heat treatments on selenium content and speciation in garlic. *Journal of Food Composition and Analysis*, *70*, 54–62. https://doi.org/10.1016/j.jfca.2018.04.004

Petersen, A., Crocoll, C., & Halkier, B. A. (2019). De novo production of benzyl glucosinolate in *Escherichia coli*. *Metabolic Engineering*, *54*, 24–34. https://doi.org/10.1016/j.ymben.2019.02.004

Pilon-Smits, E. A. (2019). On the ecology of selenium accumulation in plants. *Plants*, *8*(7), 197. https://doi.org/10.3390/plants8070197

Pyrzynska, K., & Sentkowska, A. (2021). Selenium in plant foods: Speciation analysis, bioavailability, and factors affecting composition. *Critical Reviews in Food Science and Nutrition*, *61*(8), 1340–1352. https://doi.org/10.1080/10408398.2020.1758027

Ragab, T. I., Mehany, A. B. M., Helal, M. M., & Helmy, W. A. (2018). Antitumor and prebiotic activities of novel sulfated acidic polysaccharide from ginseng. *Biocatalysis and Agricultural Biotechnology*, *14*, 402–409.

Raics, M., Balogh, Á. K., Kishor, C., Timári, I., Medrano, F. J., Romero, A., Go, R. M., Blanchard, H., Szilágyi, L., & Kövér, E. K. (2022). Investigation of the molecular details of the interactions of selenoglycosides and human galectin-3. *International Journal of Molecular Sciences*, *23*(5), 2494. https://doi.org/10.3390/ijms23052494

Rayman, M. P. (2012). Selenium and human health. *Lancet (London, England)*, *379*(9822), 1256–1268. https://doi.org/10.1016/S0140-6736(11)61452-9

Ren, D., Tian, L., & Yang, X. (2014). Chemical characterization and antioxidant activities of the selenium-containing polysaccharides and polyphenols from *Camellia sinensis* L. green tea. *Molecules (Basel, Switzerland)*, *19*, 00–00. https://doi.org/10.3390/molecules190x0000x

Ren, Y.-Y., Sun, P.-P., Li, H.-R., & Zhu, Z.-Y. (2020). Effects of Na2SeO3 on growth, metabolism, antioxidase and enzymes involved in polysaccharide synthesis of *Cordyceps militaris*. *Process Biochemistry*, *97*, 64–71. https://doi.org/10.1016/j.procbio.2020.06.018

Rotruck, J. T., Pope, A. L., Ganther, H. E., Swanson, A., Hafeman, D. G., & Hoekstra, W. (1973). Selenium: Biochemical role as a component of glutathione peroxidase. *Science*, *179*(4073), 588–590. https://doi.org/10.1126/science.179.4073.588

Rua, R. M., Nogales, F., Carreras, O., & Ojeda, M. L. (2023). Selenium, selenoproteins and cancer of the thyroid. *Journal of Trace Elements in Medicine and Biology*, *76*, 127115. https://doi.org/10.1016/j.jtemb.2022.127115

Schwarz, K., & Foltz, C. M. (1957). Selenium as an integral part of factor 3 against dietary necrotic liver degeneration. *Journal of the American Chemical Society*, *79*(12), 3292–3293. https://doi.org/10.1021/ja01569a087

Schweizer, U., & Fabiano, M. (2022). Selenoproteins in brain development and function. *Free Radical Biology and Medicine*, *190*, 105–115. https://doi.org/10.1016/j.freeradbiomed.2022.07.022

Shi, L. (2016). Bioactivities, isolation and purification methods of polysaccharides from natural products: A review. *International Journal of Biological Macromolecules*, *92*, 37–48. https://doi.org/10.1016/j.ijbiomac.2016.06.100

Skalickova, S., Milosavljevic, V., Cihalova, K., Horky, P., Richtera, L., & Adam, V. (2017). Selenium nanoparticles as a nutritional supplement. *Nutrition (Burbank, Los Angeles County, Calif.)*, *33*, 83–90. https://doi.org/10.1016/j.nut.2016.05.001

Sun, Y., Zhou, C., Huang, S., & Jiang, C. (2017). Selenium polysaccharide SPMP-2a from *Pleurotus geesteranus* alleviates H 2 O 2-induced oxidative damage in HaCaT cells. *BioMed Research International*, *2017*, 4940384. https://doi.org/10.1155/2017/4940384

Thomson, C. D. (2004). Selenium and iodine intakes and status in New Zealand and Australia. *British Journal of Nutrition*, *91*(5), 661–672. https://doi.org/10.1079/BJN20041110

Ventura, M., Melo, M., & Carrilho, F. (2017). Selenium and thyroid disease: From pathophysiology to treatment. *International Journal of Endocrinology*, *2017*, 1297658. https://doi.org/10.1155/2017/1297658

Wadhwani, S. A., Shedbalkar, U. U., Singh, R., & Chopade, B. A. (2016). Biogenic selenium nanoparticles: Current status and future prospects. *Applied Microbiology and Biotechnology*, *100*(6), 2555–2566. https://doi.org/10.1007/s00253-016-7300-7

Wang, H., Shi, S., Gu, X., Zhu, C., Wei, G., Wang, H., Bao, B., Fan, H., Zhang, W., & Duan, J. (2013). Homogalacturonans from preinfused green tea: Structural characterization and anticomplementary activity of their sulfated derivatives. *Journal of Agricultural and Food Chemistry*, *61*(46), 10971–10980. https://doi.org/10.1021/jf401947n

Wang, J., Zhao, B., Wang, X., Yao, J., & Zhang, J. (2012). Synthesis of selenium-containing polysaccharides and evaluation of antioxidant activity in vitro. *International Journal of Biological Macromolecules*, *51*(5), 987–991. https://doi.org/10.1016/j.ijbiomac.2012.08.011

Wang, S., Liang, D., Wang, D., Wei, W., Fu, D., & Lin, Z. (2012). Selenium fractionation and speciation in agriculture soils and accumulation in corn (*Zea mays* L.) under field conditions in Shaanxi Province, China. *Science of the Total Environment*, *427*, 159–164. https://doi.org/10.1016/j.scitotenv.2012.03.091

Wang, S., Wu, H., Zhang, X., Luo, S., Zhou, S., Fan, H., & Lv, C. (2023). Preparation of nano-selenium from chestnut polysaccharide and characterization of its antioxidant activity. *Frontiers in Nutrition*, *9*, 1054601. https://doi.org/10.3389/fnut.2022.1054601

Wang, Y., Chen, J., Zhang, D., Zhang, Y., Wen, Y., Li, L., & Zheng, L. (2013). Tumoricidal effects of a selenium (Se)-polysaccharide from Ziyang green tea on human osteosarcoma U-2 OS cells. *Carbohydrate Polymers*, *98*(1), 1186–1190. https://doi.org/10.1016/j.carbpol.2013.07.022

Wang, Y., Li, Y., Liu, Y., Chen, X., & Wei, X. (2015). Extraction, characterization and antioxidant activities of Se-enriched tea polysaccharides. *International Journal of Biological Macromolecules*, *77*, 76–84. https://doi.org/10.1016/j.ijbiomac.2015.02.052

Wang, Z., Wang, X., Xiu, W., & Ma, Y. (2022). Characteristics of selenium polysaccharide from sweet corncob and its effects on non-enzymatic glycosylation in vivo. *Applied Biological Chemistry*, *65*(1), 10.

Wei, Y., Zhao, Q., Wu, Q., Zhang, H., Kong, W., Liang, J., Yao, J., Zhang, J., & Wang, J. (2019). Efficient synthesis of polysaccharide with high selenium content mediated by imidazole-based acidic ionic liquids. *Carbohydrate Polymers*, *203*, 157–166.

Wu, Z., Lei, Z., Zeng, W., & Yang, J. (2023). Effect of tea polysaccharides on faecal microbiota and their short-chain fatty acid metabolic products. *International Food Research Journal*, *30*(1), 151–162. https://doi.org/10.47836/ifrj.30.1.12

Xiang, A., Li, W., Zhao, Y., Ju, H., Xu, S., Zhao, S., Yue, T., & Yuan, Y. (2022). Purification, characterization and antioxidant activity of selenium-containing polysaccharides from pennycress (*Thlaspi arvense* L.). *Carbohydrate Research*, *512*, 108498. https://doi.org/10.1016/j.carres.2021.108498

Xiao, H., Chen, C., Li, C., Huang, Q., & Fu, X. (2019). Physicochemical characterization, antioxidant and hypoglycemic activities of selenized polysaccharides from *Sargassum pallidum*. *International Journal of Biological Macromolecules*, *132*, 308–315. https://doi.org/10.1016/j.ijbiomac.2019.03.138

Yamashita, M., Yamashita, Y., Suzuki, T., Kani, Y., Mizusawa, N., Imamura, S., Takemoto, K., Hara, T., Hossain, M. A., Yabu, T., & Touhata, K. (2013). Selenoneine, a novel selenium-containing compound, mediates detoxification mechanisms against methylmercury accumulation and toxicity in zebrafish embryo. *Marine Biotechnology (New York, N.Y.)*, *15*(5), 559–570. https://doi.org/10.1007/s10126-013-9508-1

Yamashita, Y., & Yamashita, M. (2010). Identification of a novel selenium-containing compound, selenoneine, as the predominant chemical form of organic selenium in the blood of bluefin tuna. *Journal of Biological Chemistry*, *285*(24), 18134–18138. https://doi.org/10.1074/jbc.C110.106377

Yang, J., Du, Y., Huang, R., Wan, Y., & Wen, Y. (2005). The structure–anticoagulant activity relationships of sulfated lacquer polysaccharide: Effect of carboxyl group and position of sulfation. *International Journal of Biological Macromolecules*, *36*(1-2), 9–15. https://doi.org/10.1016/j.ijbiomac.2005.03.002

Yang, W., Huang, G., Chen, F., & Huang, H. (2021). Extraction/synthesis and biological activities of selenopolysaccharide. *Trends in Food Science & Technology*, *109*, 211–218. https://doi.org/10.1016/j.tifs.2021.01.0282011

Yang, Y., Liu, D., Wu, J., Chen, Y., & Wang, S. (2011). In vitro antioxidant activities of sulfated polysaccharide fractions extracted from Corallina officinalis. *Int J Biol Macromol*, *49*(5), 1031–1037. https://doi.org/10.1016/j.ijbiomac.2011.08.026

Yuan, B., Yang, X.-Q., Kou, M., Lu, C.-Y., Wang, Y.-Y., Peng, J., Chen, P., & Jiang, J.-H. (2017). Selenylation of polysaccharide from the sweet potato and evaluation of antioxidant, antitumor, and antidiabetic activities. *Journal of Agricultural and Food Chemistry*, *65*(3), 605–617. https://doi.org/10.1021/acs.jafc.6b04788

Zagrodzki, P., Pasko, P., Domínguez-Álvarez, E., Salardón-Jiménez, N., Sevilla-Hernández, C., Sanmartín, C., Bierła, K., Łobiński, R., Szpunar, J., Handzlik, J., Jacob, C., Bieniek, U., Galanty, A., & Gorinstein, S. (2022). Synthesis of novel organic selenium compounds and speciation of their metabolites in biofortified kale sprouts. *Microchemical*, *172*, 106962. https://doi.org/10.1016/j.microc.2021.106962

Zainudin, N., Hemly, N., Muhammad, A., Nayan, N., & Samsudin, A. (2023). Effects of supplementing organic-and inorganic-based selenium with vitamin E on intestinal histomorphology, caecal bacterial proliferation, and short-chain fatty acid profile in layer hens. *Tropical Animal Health and Production*, *55*(2), 90. https://doi.org/10.1007/s11250-023-03482-x

Zhang, H., & Chen, K. (2012). Biophysical studies on the site-selective binding of a synthesized selenium–quercetin complex on a protein. *Journal of Solution Chemistry*, *41*(6), 915–925. https://doi.org/10.1007/s10953-012-9844-1

Zhang, H., Zhao, Z., Zhang, X., Zhang, W., Huang, L., Zhang, Z., Yuan, L., & Liu, X. (2019). Effects of foliar application of selenate and selenite at different growth stages on selenium accumulation and speciation in potato (*Solanum tuberosum* L.). *Food Chemistry*, *286*, 550–556. https://doi.org/10.1016/j.foodchem.2019.01.185

Zhang, L., Hu, B., Li, W., Che, R., Deng, K., Li, H., Yu, F., Ling, H., Li, Y., & Chu, C. (2014). Os PT 2, a phosphate transporter, is involved in the active uptake of selenite in rice. *New Phytologist*, *201*(4), 1183–1191. https://doi.org/10.1111/nph.12596

Zhang, Y., Zhang, Z., Liu, H., Wang, D., Wang, J., Deng, Z., Li, T., He, Y., Yang, Y., & Zhong, S. (2020). Physicochemical characterization and antitumor activity in vitro of a selenium polysaccharide from *Pleurotus ostreatus*. *International Journal of Biological Macromolecules*, *165*(Pt B), 2934–2946. https://doi.org/10.1016/j.ijbiomac.2020.10.168

Zhang, Y., Zhang, Z., Liu, H., Wang, D., Wang, J., Liu, M., Yang, Y., & Zhong, S. (2022). A natural selenium polysaccharide from *Pleurotus ostreatus*: Structural elucidation, anti-gastric cancer and anti-colon cancer activity in vitro. *International Journal of Biological Macromolecules*, *201*, 630–640. https://doi.org/10.1016/j.ijbiomac.2022.01.101

Zhang, Z., Zhang, Y., Liu, H., Wang, J., Wang, D., Deng, Z., Li, T., He, Y., Yang, Y., & Zhong, S. (2021). A water-soluble selenium-enriched polysaccharide produced by *Pleurotus ostreatus*: Purification, characterization, antioxidant and antitumor activities in vitro. *International Journal of Biological Macromolecules*, *168*, 356–370. https://doi.org/10.1016/j.ijbiomac.2020.12.070

Zhao, Y., Chen, H., Li, W., He, Q., Liang, J., Yan, X., Yuan, Y., & Yue, T. (2022). Selenium-containing tea polysaccharides ameliorate DSS-induced ulcerative colitis via enhancing the intestinal barrier and regulating the gut microbiota. *International Journal of Biological Macromolecules*, *209*(Pt A), 356–366. https://doi.org/10.1016/j.ijbiomac.2022.04.028

Zhou, L., Li, Y., Gong, X., Li, Z., Wang, H., Ma, L., Tuerhong, M., Abudukeremu, M., Ohizumi, Y., & Xu, J. (2022). Preparation, characterization, and antitumor activity of Chaenomeles speciosa polysaccharide-based selenium nanoparticles. *Arabian Journal of Chemistry*, *15*(8), 103943.

Zhou, N., Long, H., Wang, C., Zhu, Z., Yu, L., Yang, W., Ren, X., & Liu, X. (2020). Characterization of selenium-containing polysaccharide from *Spirulina platensis* and its protective role against Cd-induced toxicity. *International Journal of Biological Macromolecules*, *164*, 2465–2476. https://doi.org/10.1016/j.ijbiomac.2020.08.100

Zhu, J., Chen, Z., Chen, L., Yu, C., Wang, H., Wei, X., & Wang, Y. (2019). Comparison and structural characterization of polysaccharides from natural and artificial Se-enriched green tea. *International Journal of Biological Macromolecules*, *130*, 388–398. https://doi.org/10.1016/j.ijbiomac.2019.02.102

Zhu, J., Yu, C., Han, Z., Chen, Z., Wei, X., & Wang, Y. (2020). Comparative analysis of existence form for selenium and structural characteristics in artificial selenium-enriched and synthetic selenized green tea polysaccharides. *International Journal of Biological Macromolecules*, *154*, 1408–1418. https://doi.org/10.1016/j.ijbiomac.2019.11.022

Zhu, S., Hu, J., Liu, S., Guo, S., Jia, Y., Li, M., Kong, W., Liang, J., Zhang, J., & Wang, J. (2020). Synthesis of Se-polysaccharide mediated by selenium oxychloride: Structure features and antiproliferative activity. *Carbohydrate Polymers*, *246*, 116545. https://doi.org/10.1016/j.carbpol.2020.116545

How to cite this article: Qi, Z., Duan, A., & Ng, K. (2024). Selenosugar, selenopolysaccharide, and putative selenoflavonoid in plants. *Comprehensive Reviews in Food Science and Food Safety*, *23*, e13329. https://doi.org/10.1111/1541-4337.13329